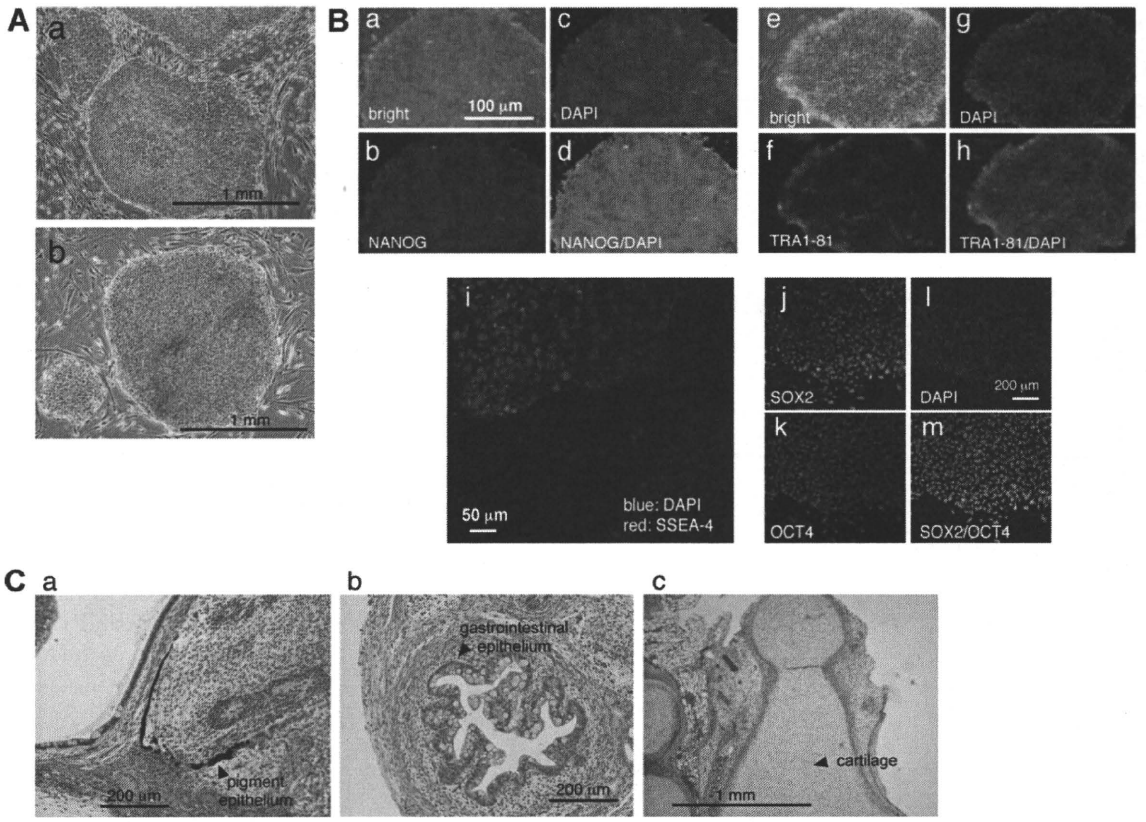

Figure 7. Culture of cynomolgus monkey ES cells on dishes coated with the α1(I) chain. **A**: Appearance of monkey ES cells. Cynomolgus monkey ES cells were cultured on feeder cells that had been cultured on dishes coated with the α1(I) chain (**a**) or porcine gelatin (**b**). Scale bar, 1 mm. **B**: Immunostain of the ES cell colonies. ES cell colonies were analyzed for the expression of marker proteins. **Panels (a–d** and **e–h)** show colonies immunostained with anti-NANOG and TRA1-81 antibodies, respectively. **Panels (a)** and **(e)**: appearances in bright fields; **panels (b)** and **(f)**: immunostained signals; **panels (c)** and **(g)**: DAPI-stained signals; **panels (d)** and **(h)**: mergers of immunostained and DAPI-stained signals. **Panel (i)** represents a colony stained with the anti-SSEA-4 antibody and DAPI. **Panels (j–m)** show a colony double-stained with anti-SOX2 and OCT4 antibodies. **Panel (j)**: immunostained signal with anti-SOX2 antibody; **panel (k)**: immunostained signal with anti-OCT4 antibody; **panel (l)**: DAPI-stained signal; **panel (m)**: merger of signals with anti-SOX2 and those with OCT4 antibodies. Scale bars, **(a)**: 100 μm; **(i)**: 50 μm; **(l)**: 200 μm. **C**: Teratoma formation in SCID mice. The ES cells were injected subcutaneously into the hind leg of SCID mice. Sections of the teratomas that formed were stained with hematoxylin and eosin. Arrowheads in **(a–c)** point to the pigment epithelium, gastrointestinal epithelium, and cartilage, respectively. Scale bars, **(a)** and **(b)**: 200 μm; **(c)**: 1 mm.

α5β1 indirectly recognizes it via collagen-bound fibronectin (Mould et al., 1997). Although the detailed mechanism is unknown, the complete absence of hydroxyprolines or the triple helical structure in the α1(I) chain may be responsible for this discrimination. At concentrations >5.0 μg/mL, however, HSFs spread on the α1(I) chain at a similar rate to that of gelatin. At a concentration of 10 μg/mL, the cell morphology was indistinguishable from that on collagen or gelatin. These results emphasize the practical utility of the recombinant α1(I) chain as a cell scaffold.

To demonstrate the practicality of the α1(I) chain, monkey ES cells were cultured on chain-coated dishes. After 30 passages, the monkey ES cell colonies maintained excellent morphology and the expression of several marker proteins for ES cells. The pluripotency of the cells was also confirmed by the formation of teratomas in SCID mice.

Gelatins are generally used for culturing ES or iPS cells. However, most marketed gelatins are derived from bovine or porcine bone, and therefore there is a risk of contamination with animal-derived pathogens, including viruses. In contrast, the recombinant α1(I) chain developed in this study does not pose such a risk because the chain is extracted from silk cocoons without using animal-derived materials. In addition, the α1(I) chain is composed of human sequences with constant molecular weight. Unlike the animal-derived gelatin extracted by hydrolyzing tissue collagens, the quality of the chain can be easily controlled with lot-to-lot consistency. The endotoxin level of the α1(I) chain was much lower than marketed gelatins. The recombinant α1(I) chain is a promising candidate material for use as a high-quality gelatin substitute for tissue engineering, drug delivery, and other applications.

References

Adachi T, Tomita M, Yoshizato K. 2005. Synthesis of prolyl 4-hydroxylase α subunit and type IV collagen in hemocytic granular cells of silkworm,

Bombyx mori: Involvement of type IV collagen in self-defense reaction and metamorphosis. Matrix Biol 24:136–154.

Adachi T, Tomita M, Shimizu K, Ogawa S, Yoshizato K. 2006. Generation of hybrid transgenic silkworms that express *Bombyx mori* prolyl-hydroxylase alpha-subunits and human collagens in posterior silk glands: Production of cocoons that contained collagens with hydroxylated proline residues. J Biotechnol 126:205–219.

Berg RA, Prockop DJ. 1973. The thermal transition of a non-hydroxylated form of collagen. Evidence for a role for hydroxyproline in stabilizing the triple-helix of collagen. Biochem Biophys Res Commun 52:115–120.

Bradley R. 1993. The research programme on transmissible spongiform encephalopathies in Britain with special reference to bovine spongiform encephalopathy. Dev Biol Stand 80:157–170.

Cameron CM, Hu WS, Kaufman DS. 2006. Improved development of human embryonic stem cell-derived embryoid bodies by stirred vessel cultivation. Biotechnol Bioeng 94:938–948.

Doege KJ, Fessler JH. 1986. Folding of carboxyl domain and assembly of procollagen I. J Biol Chem 261:8924–8935.

Fichard A, Tillet E, Delacoux F, Garron R, Ruggiero F. 1997. Human recombinant alpha1(V) collagen chain. Homotrimeric assembly and subsequent processing. J Biol Chem 272:30083–30087.

Garel A, Deleage G, Prudhomme JC. 1997. Structure and organization of the *Bombyx mori* sricin 1 gene and of the sericins 1 deduced from the sequence of the Ser 1B cDNA. Insect Biochem Mol Biol 27:469–477.

Geddis AE, Prockop DJ. 1993. Expression of human COL1A1 gene in stably transfected HT1080 cells: The production of a thermostable homotrimer of type I collagen in a recombinant system. Matrix 13:399–405.

Gill J, Feinberg J. 2001. Saquinavir soft gelatin capsule: A comparative safety review. Drug Saf 24:223–232.

Grzelak K. 1995. Control of expression of silk protein genes. Comp Biochem Physiol 110:671–681.

Hynes RO. 2002. Integrins: Bidirectional, allosteric signaling machines. Cell 110:673–687.

Iizuka M, Tomita M, Shimizu K, Kikuchi Y, Yoshizato K. 2008. Translational enhancement of recombinant protein synthesis in transgenic silkworms by a 5'-untranslated region of polyhedrin gene of *Bombyx mori* Nucleopolyhedrovirus. J Biosci Bioeng 105:595–603.

Iizuka M, Ogawa S, Takeuchi A, Nakakita S, Kubo Y, Miyawaki Y, Hirabayashi J, Tomita M. 2009. Production of a recombinant mouse monoclonal antibody in transgenic silkworm cocoons. FEBS J 276:5806–5820.

John DC, Watson R, Kind AJ, Scott AR, Kadler KE, Bulleid NJ. 1999. Expression of an engineered form of recombinant procollagen in mouse milk. Nat Biotechnol 17:385–389.

Lamberg A, Helaakoski T, Myllyharju J, Peltonen S, Notbohm H, Pihlajaniemi T, Kivirikko KI. 1996. Characterization of human type III collagen expressed in a baculovirus system. Production of a protein with a stable triple helix requires coexpression with the two types of recombinant prolyl 4-hydroxylase subunit. J Biol Chem 271:11988–11995.

Lee CH, Singla A, Lee Y. 2001. Biomedical applications of collagen. Int J Pharm 221:1–22.

Lin MS, Alfi OS, Donnell GN. 1976. Differential fluorescence of sister chromatids with 4'-6-diamidino-2-phenylindole. Can J Genet Cytol 18:545–547.

Merle C, Perret S, Lacour T, Jonval V, Hudaverdian S, Garrone R, Ruggiero F, Theisen M. 2002. Hydroxylated human homotrimeric collagen I in Agrobacterium tumefaciens-mediated transient expression and in transgenic tobacco plant. FEBS Lett 515:114–118.

Michalopoulos G, Pitot HC. 1975. Primary culture of parenchymal liver cells on collagen membranes. Morphological and biochemical observations. Exp Cell Res 94:70–78.

Miller EJ, Gay S. 1982. The collagens: An overview and update. Methods Enzymol 82:3–32.

Miyata T, Taira T, Noishiki Y. 1992. Collagen engineering for biomaterial use. Clin Mater 9:139–148.

Mould AP, Askari JA, Aota S, Yamada KM, Irie A, Takada Y, Mardon HJ, Humphries MJ. 1997. Defining the topology of integrin alpha5 beta1-fibronectin interactions using inhibitory anti-alpha5 and anti-beta1 monoclonal antibodies. Evidence that the synergy sequence of fibronectin is recognized by the amino-terminal repeats of the alpha5 subunit. J Biol Chem 272:17283–17292.

Mullins RJ, Richards C, Walker T. 1996. Allergic reactions to oral, surgical and topical bovine collagen. Anaphylactic risk for surgeons. Aust NZ J Ophthalmol 24:257–260.

Nicholls AC, Pope FM, Schloon H. 1979. Biochemical heterogeneity of osteogenesis imperfecta: New variant. Lancet 1:1193.

Ogawa S, Tomita M, Shimizu K, Yoshizato K. 2007. Generation of a transgenic silkworm that secretes recombinant proteins in the sericin layer of cocoon: Production of recombinant human serum albumin. J Biotechnol 128:531–544.

Olsen DR, Leigh SD, Chang R, McMullin H, Ong W, Tai E, Chisholm G, Birk DE, Berg RA, Hitzeman RA, Toman PD. 2001. Production of human type I collagen in yeast reveals unexpected new insights into the molecular assembly of collagen trimers. J Biol Chem 276:24038–24043.

Olsen D, Yang C, Bodo M, Chang R, Leigh S, Baez J, Carmichael D, Perala M, Hamalainen ER, Jarvinen M, Polarek J. 2003. Recombinant collagen and gelatin for drug delivery. Adv Drug Del Rev 55:1547–1567.

Peltonen L, Palotie A, Hayashi T, Prockop DJ. 1980. Thermal stability of type I and type III procollagens from normal human fibroblasts and from a patient with osteogenesis imperfecta. Proc Natl Acad Sci U S A 77:162–166.

Rosenbloom J, Endo R, Harsch M. 1976. Termination of procollagen chain synthesis by puromycin. Evidence that assembly and secretion require a COOH-terminal extension. J Biol Chem 251:2070–2076.

Ruggiero F, Exposito JY, Bournat P, Gruber V, Perret S, Comte J, Olagnier B, Garrone R, Theisen M. 2000. Triple helix assembly and processing of human collagen produced in transgenic tobacco plants. FEBS Lett 469:132–136.

Suemori H, Tada T, Torii R, Hosoi Y, Kobayashi K, Imahie H, Kondo Y, Iritani A, Nakatsuji N. 2001. Establishment of embryonic stem cell lines from cynomolgus monkey blastocysts produced by IVF or ICSI. Dev Dyn 222:273–279.

Tabata Y, Ikada Y. 1998. Protein release from gelatin matrices. Adv Drug Deliv Rev 31:287–301.

Tamura T, Thibert C, Royer C, Kanda T, Abraham E, Kamba M, Komoto N, Thomas JL, Mauchamp B, Chavancy G, Shirk P, Fraser M, Prudhomme JC, Couble P. 2000. Germline transformation of the silkworm *Bombyx mori* L. using a *piggyBac* transposon-derived vector. Nat Biotechnol 18:81–84.

Tomita M, Munetsuna T, Adachi T, Hino R, Hayashi M, Shimizu K, Nakamura N, Tamura T, Yoshizato K. 2003. Transgenic silkworms produce recombinant human type III procollagen in cocoons. Nat Biotechnol 21:52–56.

Tomita M, Shimizu K, Yoshizato K. 2005. Transgenic silkworms that weave recombinant human collagen in cocoons. In: Yoshizato K, editor. Transgenic silkworms: Eurekah Bioscience Collection. Georgetown: Landes Bioscience. chapter 2657.

Tomita M, Hino R, Ogawa S, Iizuka M, Adachi T, Shimizu K, Sotoshiro H, Yoshizato K. 2007. A germline transgenic silkworm that secretes recombinant proteins in the sericin layer of cocoon. Transgenic Res 16:449–465.

Vuorela A, Myllyharju J, Nissi R, Pihlajaniemi T, Kivirikko KI. 1997. Assembly of human prolyl 4-hydroxylase and type III collagen in the yeast *Pichia pastoris*: Formation of a stable enzyme tetramer requires coexpression with collagen and assembly of a stable collagen requires coexpression with prolyl 4-hydroxylase. EMBO J 16:6702–6712.

Werten MW, van den Bosch TJ, Wind RD, Mooibroek H, de Wolf FA. 1999. High-yield secretion of recombinant gelatins by *Pichia pastoris*. Yeast 15:1087–1096.

Yamada KM, Kennedy DW. 1984. Dualistic nature of adhesion protein function: Fibronectin and its biologically active peptide fragments can autoinhibit fibronectin function. J Cell Biol 99:29–36.

The American Journal of Pathology, Vol. 176, No. 4, April 2010

DOI: 10.2353/ajpath.2010.090486

Tumorigenesis and Neoplastic Progression

Function of *EWS-POU5F1* in Sarcomagenesis and Tumor Cell Maintenance

Takashi Fujino,*† Kimie Nomura,‡ Yuichi Ishikawa,‡ Hatsune Makino,§ Akihiro Umezawa,§ Hiroyuki Aburatani,¶ Koichi Nagasaki,‖ and Takuro Nakamura*

From the Divisions of Carcinogenesis, and Pathology,‡ and the Genome Center,‖ The Cancer Institute, Japanese Foundation for Cancer Research, Tokyo; the Department of Pathology,† Faculty of Medicine, Kyorin University, Tokyo; the Department of Reproductive Biology,§ National Institute for Child and Health Development, Tokyo; and the Genome Research Division,¶ Research Center for Advanced Science and Technology, University of Tokyo, Tokyo, Japan*

POU5F1 is a transcription factor essential for the self-renewal activity and pluripotency of embryonic stem cells and germ cells. We have previously reported that *POU5F1* is fused to *EWSR1* in a case of undifferentiated sarcoma with chromosomal translocation t(6;22)(p21;q12). In addition, the *EWS-POU5F1* chimeras have been recently identified in human neoplasms of the skin and salivary glands. To clarify the roles of the *EWS-POU5F1* chimera in tumorigenesis and tumor cell maintenance, we used small-interfering RNA-mediated gene silencing. Knockdown of *EWS-POU5F1* in the t(6;22) sarcoma-derived GBS6 cell line resulted in a significant decrease of cell proliferation because of G1 cell cycle arrest associated with $p27^{Kip1}$ up-regulation. Moreover, senescence-like morphological changes accompanied by actin polymerization were observed. In contrast, *EWS-POU5F1* down-regulation markedly increased the cell migration and invasion as well as activation of metalloproteinase 2 and metalloproteinase 14. The results indicate that the proliferative activity of cancer cells and cell motility are discrete processes in multistep carcinogenesis. These findings reveal the functional role of the sarcoma-related chimeric protein as well as POU5F1 in the development and progression of human neoplasms. *(Am J Pathol 2010, 176:1973–1982; DOI: 10.2353/ajpath.2010.090486)*

POU5F1/OCT4 is an essential transcription factor for the formation and/or maintenance of the inner cell mass of the mammalian blastocyst, the origin of pluripotent embryonic stem (ES) cells.[1–3] Suppression of *POU5F1* expression converts ES cells to trophoblasts, whereas overexpression of *POU5F1* leads to differentiation toward endoderm and mesoderm.[3,4] The self-renewal activity and pluripotency of ES cells are suppressed by knockdown of *POU5F1*.[5] These data suggest that POU5F1 orchestrates target gene expression in a tightly regulated manner during development and cellular differentiation. Also, POU5F1 induces reprogramming of somatic cells into iPS cells in combination with Sox2, c-Myc, and Klf4.[6] Moreover, two factors, either POU5F1 and Klf4 or POU5F1 and c-Myc, are apparently sufficient to generate iPS cells.[7]

In carcinogenesis, up-regulated expression of *POU5F1* is significantly correlated to certain lineages of human malignancies including germ cell tumors and breast and bladder cancer.[8–11] Reactivation of POU5F1 in somatic cells may induce dedifferentiation and may disrupt homeostasis, resulting in malignant transformation. Direct involvement of POU5F1 has been detected in a case of undifferentiated bone sarcoma with t(6;22)(p21;q12) translocation in which *POU5F1* is fused to *EWSR1*.[12] The chimeric *EWS-POU5F1* protein is composed of a transactivation domain of EWS and the entire DNA-binding domain of POU5F1. Ectopic overexpression of the POU5F1 component is achieved by the strong promoter activity of *EWSR1*.[12] Similar gene fusions between *EWSR1* and *POU5F1* have been identified in hidradenoma of the skin and mucoepidermoid carcinoma of the salivary glands.[13] These results underscore the important role of dysregulated *POU5F1* expression in human cancer and the important contributions of *EWS-POU5F1* to the development and maintenance of cancer cells.

In this study, we knocked down *EWS-POU5F1* by using *POU5F1*-specific small-interfering RNAs (siRNAs) in

Supported in part by Grant-in-Aid for Scientific Research on Priority Areas "Integrative Research Toward the Conquest of Cancer" from the Ministry of Education, Culture, Sports, Science, and Technology of Japan, and supported by Kawano Masanori Memorial Foundation for Promotion of Pediatrics.

Accepted for publication December 15, 2009.

Supplemental material for this article can be found on *http://ajp.amjpathol.org*.

Address reprint requests to Takuro Nakamura, M.D., Ph.D., Division of Carcinogenesis, The Cancer Institute, Japanese Foundation for Cancer Research, 3-8-31 Ariake, Koto-ku, Tokyo 135-8550, Japan. E-mail: takuro-ind@umin.net.

the GBS6 cell line established from the t(6;22) undifferentiated sarcoma.[12] Cellular growth was significantly suppressed by *EWS-POU5F1* depletion and was accompanied by up-regulation of $p27^{Kip1}$ expression, and senescence-like morphological alterations were observed. On the other hand, cell motility and invasive capacity were dramatically increased, and promotion of actin polymerization and activation of metalloproteinase (MMP)14 and MMP2 were observed. These results suggest that EWS-POU5F1 promotes proliferation of cancer cells but is dispensable for or even inhibits cell motility and invasiveness. This study provides important insights into EWS-POU5F1 function in carcinogenesis and tumor cell maintenance.

Materials and Methods

Cell Culture

The GBS6 cell line was established from a pelvic bone undifferentiated sarcoma with t(6;22)(p21;q12).[12] The cells were maintained at 37°C under 5% CO_2 in RPMI 1640 medium supplemented with 10% fetal bovine serum and 10 mmol/L of HEPES buffer, pH7.4. NIH3T3, HeLa, and HCT116 cells were grown at 37°C under 5% CO_2 in Dulbecco's modified Eagle's medium supplemented with 10% fetal bovine serum.

RNA Interference and DNA Transfection

RNA interference and DNA transfection experiments were performed by using Lipofectamine 2000 (Invitrogen, Carlsbad, CA). GBS6 cells were seeded on 12-well plates 24 hours before transfection at a density of 1×10^5 or 2.5×10^5 cells per well for siRNAs or plasmid DNAs, respectively. GBS6 cells were then transfected with 60 pmol or 1.6 μg of siRNAs or plasmids, respectively. The following siRNAs were purchased from Qiagen (Hilden, Germany): siRNA-POU5F1-1 (SI00690389) and siRNA-POU5F1-2 (SI026617) and control (non-sil). A FLAG-tagged p27 expression plasmid was a kind gift from Dr. Kei-ichi Nakayama.

Senescence-Associated β-galactosidase Assay

Senescence-associated β-galactosidase was detected histochemically by using a Senescence Detection Kit (Biovision, Mountain View, CA) 4 days after transfection of siRNAs.

Western Blotting

Whole cell lysates were size-fractionated by SDS-polyacrylamide gel electrophoresis and were transferred onto a nitrocellulose membrane. The membrane was blocked with Tris-buffered saline (pH 7.5) containing 0.2% Tween 20 and 5% nonfat dry milk. Primary antibodies used were as follows: goat anti-Oct3/4 (1:500 dilution; C-20, Santa Cruz Biotechnology, Santa Cruz, CA), mouse anti-lamin A/C (1:500 dilution; Santa Cruz Biotechnology), rabbit anti-p27 (1:200 dilution; Santa Cruz Biotechnology), mouse anti-p53 (1:200 dilution; DO-1, Santa Cruz Biotechnology), mouse anti-p21 (1:100 dilution; BD Biosciences, San Diego, CA), mouse anti-Rb (1:500 dilution; IF8, Santa Cruz Biotechnology), rabbit anti-Phospho-Rb (Ser807/811; 1:500 dilution; Cell Signaling Technology, Beverly, MA), mouse anti-cyclin D1 (1:500 dilution; A-12, Santa Cruz Biotechnology), rabbit anti-CDK2 (1:500 dilution; M2, Santa Cruz Biotechnology), rabbit anti-CDK4 (1:500 dilution; H-22, Santa Cruz Biotechnology), rabbit anti-CDK6 (1:500 dilution; C-21, Santa Cruz Biotechnology), mouse anti-MMP14 (1:200 dilution; Daiichi Fine Chemical, Tokyo, Japan), and mouse anti-RhoA (1:200 dilution; Upstate Biotechnology, Temecula, CA). The signals were detected by using appropriate secondary antibodies and an enhanced chemiluminescence kit (GE Health care, Piscataway, NJ).

Flow Cytometric Analysis

Single cell suspensions were permeabilized with 0.1% triton X-100 in PBS, and 50 mg/ml of propidium iodide and 1 mg/ml of RNase A were added. The cell suspensions were then analyzed by using a FACS-calibur flow cytometer (Beckton Dickinson, Franklin Lakes, NJ) and Modifit software (Beckton Dickinson).

Cell Invasion and Migration Assays

A quantitative invasion assay was performed by using a BD BioCoat Matrigel invasion chamber with 8-μm pore size membranes (BD Biosciences) according to the manufacturer's instruction. Briefly, cells incubated with siRNAs or plasmid DNAs for 24 hours were trypsinized and resuspended at a density of 1×10^5 cells per 1 ml of RPMI without serum. Cells (5×10^5) were then loaded onto inserts of the upper chambers. RPMI with 10% fetal bovine serum was added to the lower chambers. After 24 hours of incubation, cells on the upper surface membranes were removed gently with a cotton swab. Cells on the lower surface were stained with Wright-Giemsa solutions and air-dried. Cell migration was also evaluated by using the same chambers without Matrigel by assessing the cell numbers within the lower chamber. The invading or migrating cells were counted, and images were obtained by using an Olympus BX41 microscope with a 20× objective (Olympus, Tokyo, Japan). For the wound healing assay, GBS6 cells were cultured for 48 hours after transfection of siRNAs to reach 90% confluence in 12-well plates. A linear scratch, 100 μm in width, was produced by using a plastic tip. Cells were incubated in growth medium for the indicated period. Images were photographed by using an Olympus IX70 phase contrast microscope. The distance of cell migration from the scratch line was measured in micrometers on the photographs.

Gelatin Zymography

Conditioned media from GBS6 cell cultures were harvested 48 hours after siRNA transfection, loaded on 10% gelatin gels (Invitrogen), and electrophoresed. The gels were stained with 0.25% Coomassie Blue and were destained in 5% acetic acid/10% methanol to visualize bands corresponding to the gelatinolytic activity.

Total RNA Extraction, Conventional RT-PCR, and Real-Time Quantitative RT-PCR

Total RNA extraction, reverse transcription, and RNA quantification were performed according to methods described previously.[14] Conventional RT-PCR was performed by using a Gene Amp 9700 thermal cycler (Applied Biosystems, Foster City, CA). We conducted 40 cycles of three-step PCR (95°C for 30 seconds, 55°C for 1 minute, and 72°C for 1 minute) for miR032-367 locus and 25 cycles of three-step PCR (95°C for 30 seconds, 60°C for 30 seconds, and 72°C for 30 seconds) for actin. The specific forward and reverse primers for optimal amplification were designed as follows: miR302-367 locus, 5′-GGGCTCCCTTCAACTTTAAC-3′ and 5′-ATTCTGTCATTGGCTTAACAATCCATCACC-3′; β-actin, 5′-AGGCATCCTCACCCTGAAGTACCC-3′ and 5′-GCCAGGTCCAGACGCAGG-3′. Real-time RT-PCR was performed by using a 7500 Fast Real-Time PCR System (Applied Biosystems) using the following parameters: 40 cycles of three-step PCR (95°C for 15 seconds, 60°C for 30 seconds, and 72°C for 30 seconds). The specific forward and reverse primers to produce approximately 60-bp amplicons for optimal amplification in real-time PCR were designed as follows: MMP2, 5′-CCGCAGTGACGGAAAGATGT-3′ and 5′-GCCCCACTTGCGGTCAT-3′; MMP14, 5′-CGAGAGGAAGGATGGCAAATT-3′ and 5′-AGGGACGCCTCATCAAACAC-3′; β-actin, 5′-TGGATCAGCAAGCAGGAGTATG-3′ and 5′-GCATTTGCGGTGGACGAT-3′; and miR302-367 locus, 5′-TTTGAGTGTGGTGGTTCCTACCT-3′ and 5′- AGCCAAGAACTGCACACAGTGT-3′.

Actin Staining

GBS6 cells were seeded onto four-chamber culture slides (BD Biosciences) at a density of 3000 cells per well 24 hours after transfection and were incubated for an additional 24 hours in growth medium. Cells were then fixed and stained with phalloidin-rhodamine (Invitrogen). Images were photographed by using a Leica DM6000B laser scanning microscope with a 40× objective (Leica Microsystems, Cambridge, UK).

RhoA Activity Assay

To confirm RhoA activation, the amount of RhoA-GTP bound to the Rhotekin Rho-binding domain (RBD) was determined by using the Rho Activation Assay Kit (Upstate Biotechnology). Forty-eight hours after transfection of siRNAs, whole cell lysates were incubated with Rhotekin RBD-agarose for 45 minutes at 4°C. After washing, agarose beads were resuspended in Laemmli sample buffer, boiled for 5 minutes, and subjected to immunoblotting with an anti-RhoA antibody.

Microarray

The oligonucleotide array Human Genome U133 Plus 2.0 (Affymetrix, Santa Clara, CA), composed of 38,500 human genes and expressed sequence tags, was hybridized with cRNA probes generated from GBS6 cells 4 days after siRNA transfection and was scanned according to the method previously described.[14] The data were deposited in a public database (*http://www.ncbi.nlm.nih.gov/geo*, accession number: GSE12320, last accessed November 5, 2009). Clustering analysis was performed by using dChip software (*http://biosun1.harvard.edu/complab/dchip/* last accessed October 14, 2009). The gene network was analyzed by Webgestalat (*http://bioinfo.vanderbilt.edu/webgestalt/* last accessed October 31, 2009).

Statistical Analysis

Results were evaluated statistically by using Student's *t*-test. A value of $P < 0.05$ was considered significant.

Results

EWS-POU5F1 *Knockdown Induces p27^{Kip1} Up-Regulation and G1 Arrest*

The GBS6 cell line was established from a t(6;22) undifferentiated sarcoma that expressed the chimeric *EWS-POU5F1* but not wild-type *POU5F1*.[12] To investigate the biological role of *EWS-POU5F1*, we knocked down *EWS-POU5F1* in GBS6 cells by RNA interference. Effective knockdown of *EWS-POU5F1* on 2 days after transfection was confirmed for two independent *POU5F1*-specific siRNAs (Figure 1A, 88.3% of reduction by siRNA-1 and 85.9% by siRNA-2). The effects of the two siRNAs were similar to each other in every experiment, and the results using siRNA-POU5F1-1 are exhibited subsequently as a representative.

Suppression of *EWS-POU5F1* in GBS6 cells was significantly inhibited proliferation, the cell numbers being 58% or 54% of those treated with a control siRNA on day 2 or day 4, respectively (Figure 1B). A terminal deoxynucleotidyl transferase-mediated dUTP nick-end labeling assay did not show an apparent increase of apoptotic cells during treatment with RNA interference (data not shown). This result suggests that the suppression of cell growth might be because of inhibition of the cell cycle. Flow cytometric analysis demonstrated that knockdown of *EWS-POU5F1* significantly decreased the S-phase population and increased the G1 fraction compared with the control (Figure 1C), indicating that cell growth of GBS6 was suppressed because of G1 arrest.

We next examined the expression of a series of cell cycle regulators. Increased expression of p27 was observed in GBS6 cells during *EWS-POU5F1* knockdown (Figure 1D, left). An RT-PCR experiment showed no significant decrease of *p27* mRNA during *EWS-POU5F1*

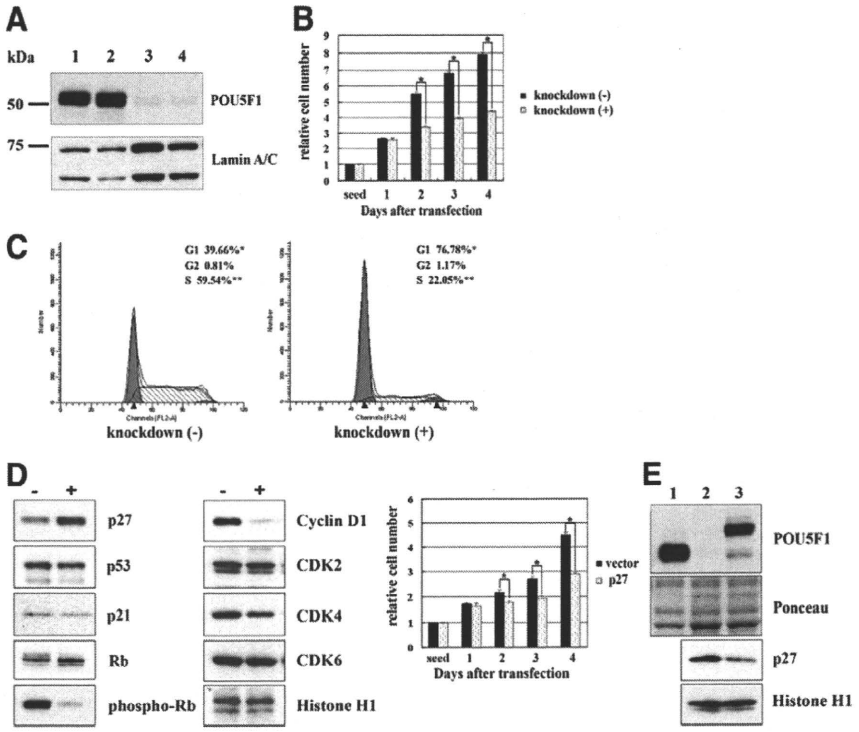

Figure 1. Knockdown of *EWS-POU5F1* inhibits proliferation of GBS6 cells accompanied by G1 cell cycle arrest and up-regulation of p27. **A:** RNA interference. GBS6 cells were transfected with control or *POU5F1* siRNAs and harvested 2 days after transfection; lysates were subjected to Western blotting by using anti-POU5F1 antibody. Lamin A/C was used as a control. **Lane 1**, wild-type; **lane 2**, negative control siRNA (non-sil); **lane 3**, POU5F1 siRNA-1; **lane 4**, POU5F1 siRNA-2. **B:** Proliferation assay of GBS6 cells treated with non-sil or POU5F1 siRNA. Mean of relative cell numbers ± SE of three independent experiments are presented ($^*P < 0.005$). **C:** Flow cytometric analysis of GBS6 cells treated with siRNAs. Average percentages of G1, G2, and S phases in three experiments are indicated. $^*P < 0.005$. **D:** Western blotting of GBS6 cells transfected with control (−) or POU5F1 (+) siRNAs by using antibodies specific for the indicated protein. Histone H1 was used as a loading control (**left**); proliferation assay (**right**) of GBS6 cells in which p27 was introduced. Mean of relative cell numbers ± SE of three independent experiments are presented (*, $^{**}P < 0.005$). **E:** Western blotting of GBS6 cells and NIH3T3 cells transfected with an empty or *EWS-POU5F1* vectors by using anti-POU5F1 or anti-p27. **Lane 1**, GBS6 cells; **lane 2**, NIH3T3 treated with an empty vector; and **lane 3**, NIH3T3 treated with an *EWS-POU5F1* expression vector. Ponceau staining and Histone H1 were used as a loading control.

suppression (data not shown), suggesting that the change might be indirect and *p27* was not transcriptionally regulated by EWS-POU5F1. During knockdown, phosphorylation of Rb protein on Ser807/811 was significantly decreased, whereas expression of total Rb protein remained unchanged (Figure 1D, left). Expression of p21 and p53 was not affected (Figure 1D, left). In addition, a comparative genomic hybridization analysis revealed a homozygous loss of $p16^{INK4A}/p14^{ARF}$ (Supplemental Figure S1, see *http://ajp.amjpathol.org*). A significant decrease of cyclin D1 expression was also noted (Figure 1D, left). On the other hand, expression of CDK2, CDK4, and CDK6 was unchanged (Figure 1D, left).

Exogenous introduction of *p27* into GBS6 cells resulted in 82% and 61% decreased proliferation compared with the transfected controls on days 2 and 4, respectively (Figure 1D, right). Conversely, exogenous expression of *EWS-POU5F1* in NIH3T3 cells markedly depleted p27 (Figure 1E). However, expression of *EWS-POU5F1* did not affect proliferation of NIH3T3 cells, suggesting that the effect might be cell context-dependent. Taken together, these results indicate that EWS-POU5F1 supports tumor cell growth, at least in part, through down-regulating the $p27^{Kip1}$ activity.

Induction of the Senescence-Like Morphology by EWS-POU5F1 *Knockdown*

GBS6 cells possess a short spindle-shaped morphology with a narrow cytoplasm and a small nucleus with rough heterochromatin (Figure 2A, left), reflecting the original phenotype *in vivo*.[12] After introduction of *POU5F1*-specific siRNAs, we observed prompt enlargement of GBS6 cell bodies. Most GBS6 cells demonstrated large and flat cytoplasms as well as enlarged nuclei with fine chromatins 4 days after siRNA transfection. This morphology mimicked that observed in cellular senescence (Figure 2A, right). Most of the GBS6 cells enlarged by *EWS-POU5F1* knockdown expressed senescence-associated β-galactosidase (Figure 2B), a well-established biomarker of senescence.[15] However, senescence-associated heterochromatin foci, another biomarker of senescence,[16] were not observed (data not shown). Importantly, the enlarged GBS6 phenotype (and growth arrest) mediated by *POU5F1*-specific siRNAs disappeared 10 days after transfection when *EWS-POU5F1* expression returned (data not shown). Thus, the change was transient and reversible. These data suggest that the phenotypic changes were not because of senescence but rather indicated G1 arrest. Interestingly, overexpression of $p27^{Kip1}$ did not induce morphological changes in GBS6 cells (data not shown), indicating that different molecular pathways downstream of EWS-POU5F1 are responsible for the senescence-like morphologies.

Drastic modification of the cytoskeleton was also observed in siRNA-treated enlarged GBS6 cells. Phalloidin staining revealed prominent networks of F-actin throughout the cytoplasm of siRNA-treated cells (Figure 2C, right). Control GBS6 cells showed only a small amount of actin fibers in the cytoplasmic rim (Figure 2C, left). A close link between actin polymerization and a small G protein Rho has been reported.[17] Indeed, a GTP-bound activated form of RhoA protein was apparently increased on *EWS-POU5F1* knockdown (Figure 2D). These data indicate that EWS-POU5F1 affected the RhoA signaling pathway and morphology of tumor cells by modulating the actin fiber network. Finally, transfection of *POU5F1*-specific siRNA into HeLa cells that do not express *POU5F1* did not affect cell morphology (Figure 2E), indi-

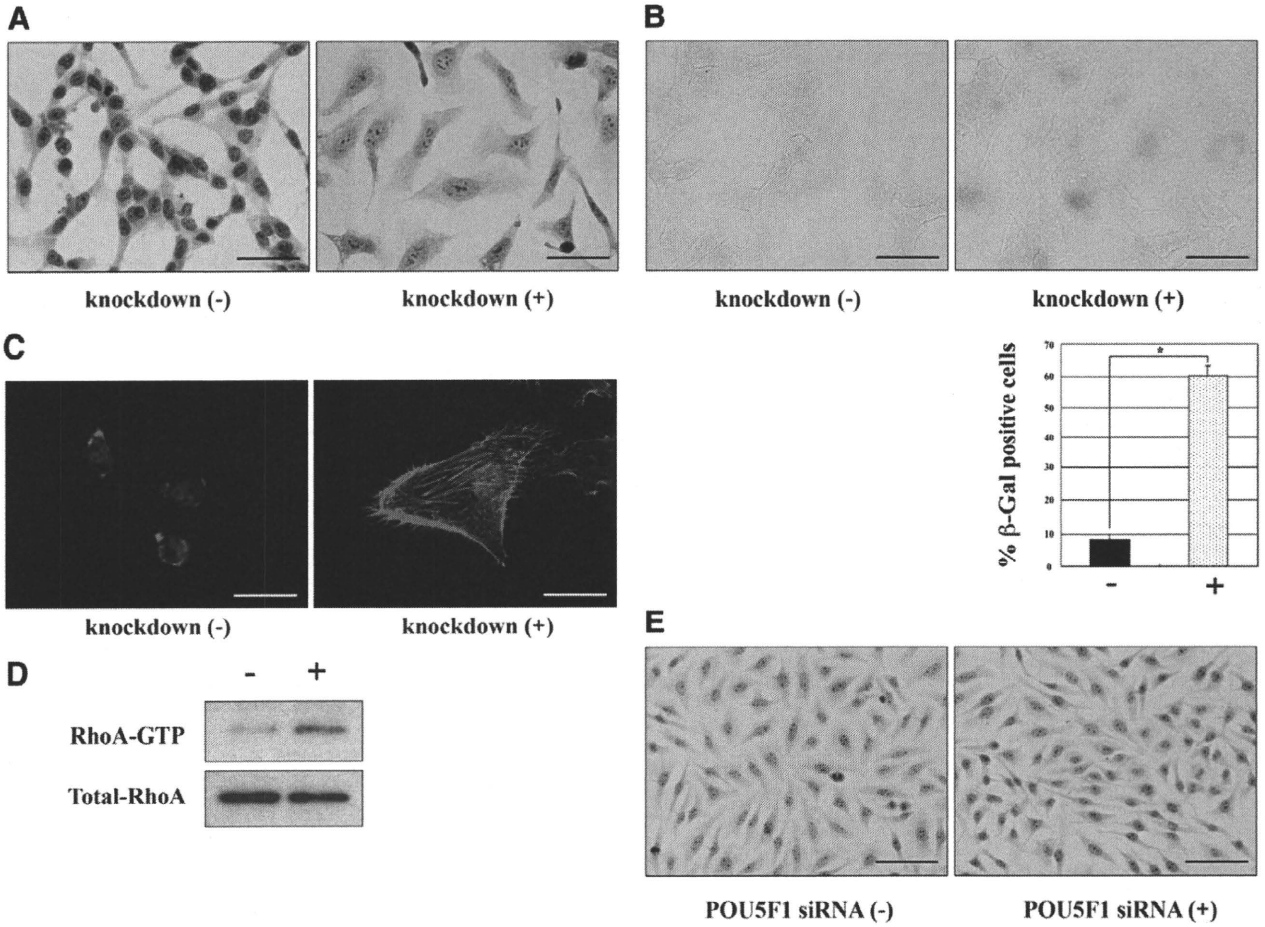

Figure 2. Morphological changes and actin polymerization in siRNA-treated GBS6 cells. **A:** Photomicrographs of GBS6 cells transfected with control siRNA or *POU5F1*-specific siRNA. Papanicolau staining, ×400 original magnification. Scale bars = 100 μm. **B:** Senescence-associated β-galactosidase (SA-β-Gal) assay 4 days after transfection of siRNAs. Original magnification, ×400. Scale bars = 100 μm. The columns indicate mean % SA-β-Gal-positive cells in three independent experiments ($^*P < 0.005$). **C:** Enhanced actin polymerization in *EWS-POU5F1* silent GBS6 cells. F-actin was visualized by phalloidin-rhodamine staining. Original magnification, ×400. Scale bars = 100 μm. **D:** Increased RhoA-GTP in *EWS-POU5F1* silenced GBS6 cells (+) compared with control (−). **E:** *POU5F1* knockdown does not affect morphology of HeLa cells. Papanicolau staining, ×200 original magnification. Scale bars = 100 μm.

cating that the above findings are not because of nonspecific effects of *POU5F1* siRNAs.

Knockdown of EWS-POU5F1 *Promotes Cell Migration and Invasion*

Uncontrolled proliferation and metastatic activities are important biological characteristics of cancer.[18] Indeed, in the t(6;22) sarcoma case, the patient died of multiple pulmonary metastases.[12] Therefore, it is intriguing to clarify whether EWS-POU5F1 promotes cell migration and invasiveness. Migration and invasion of GBS6 cells treated with siRNA for *EWS-POU5F1*were assessed in a Matrigel invasion assay. *EWS-POU5F1* knockdown resulted in marked increases in migration and invasion activities compared with the control GBS6 cells (Figure 3A and Table 1). The original GBS6 cells rarely migrated *in vitro*; however, the number of cells migrating in the absence of EWS-POU5F1 increased more than 50-fold. The increase in cell motility after *EWS-POU5F1* knockdown was also confirmed by a wound healing assay, showing that GBS6 cells with *EWS-POU5F1* knockdown migrated 2.5-fold faster than the control cells (Figure 3B).

We next asked whether the enhanced invasiveness of GBS6 cells in Matrigel was solely because of increased cell motility or whether invasiveness itself was also accelerated. Because cell invasion activity is closely associated with increased metalloproteinase activity,[19,20] MMP2 and MMP9 activities were assessed by gelatin zymography. The zymogram exhibited a significant increase of the gelatinolytic activity of MMP2, whereas the MMP9 activity was not altered (Figure 3C, top). MMP14/MT1-MMP, a membrane-type MMP, activates pro-MMP2 in collaboration with a tissue inhibitor of metalloproteinase 2.[19,21] An immunoblot analysis demonstrated increased expression of the MMP14 protein (Figure 3C, bottom), consistent with promotion of MMP2 activity. Thus, *EWS-POU5F1* knockdown increased cell motility and also enhanced invasiveness through accelerated degradation of matrix by MMPs.

Real-time quantitative RT-PCR showed that expression of MMP2 and MMP14 was also increased at the RNA level (Figure 3D), suggesting that *EWS-POU5F1* may also

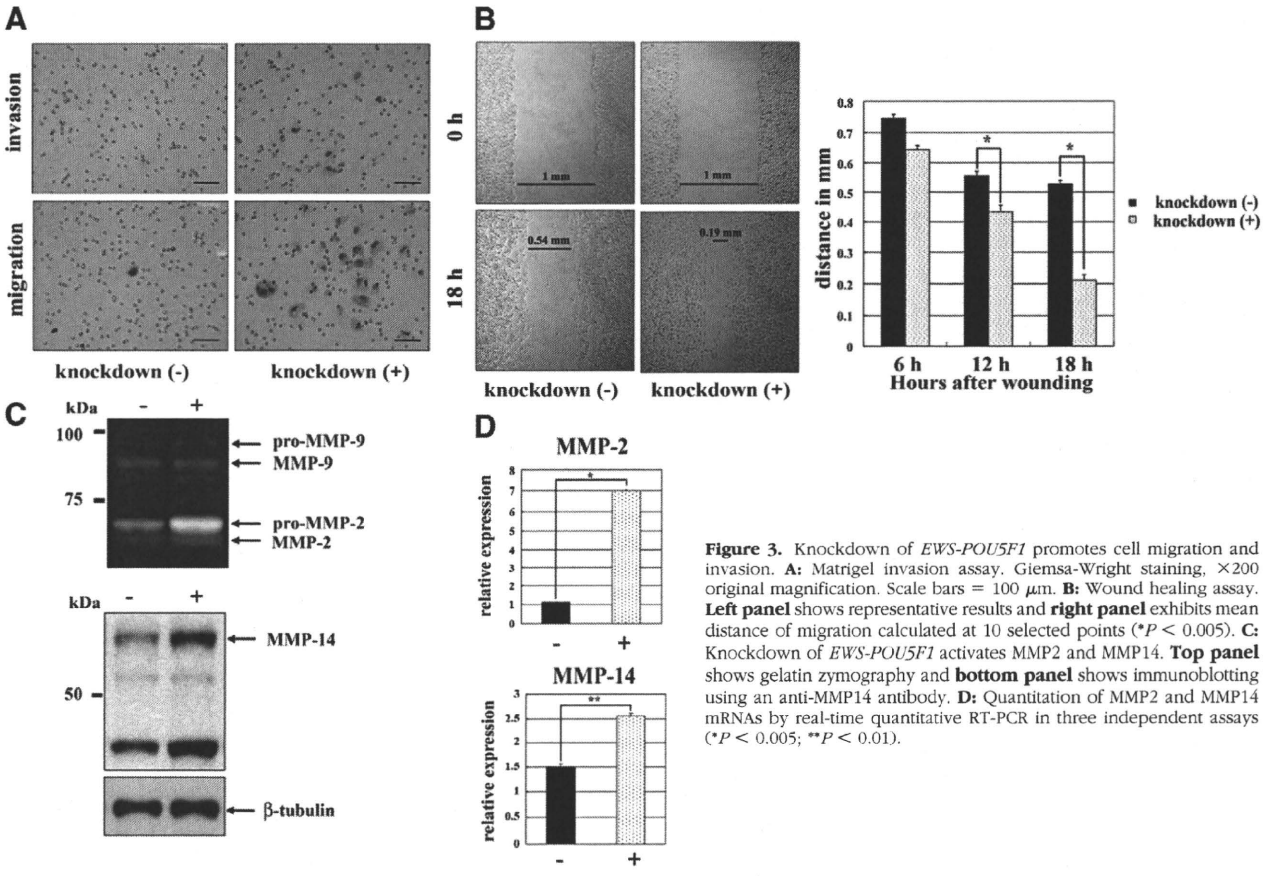

Figure 3. Knockdown of *EWS-POU5F1* promotes cell migration and invasion. **A:** Matrigel invasion assay. Giemsa-Wright staining, ×200 original magnification. Scale bars = 100 μm. **B:** Wound healing assay. **Left panel** shows representative results and **right panel** exhibits mean distance of migration calculated at 10 selected points (*$P < 0.005$). **C:** Knockdown of *EWS-POU5F1* activates MMP2 and MMP14. **Top panel** shows gelatin zymography and **bottom panel** shows immunoblotting using an anti-MMP14 antibody. **D:** Quantitation of MMP2 and MMP14 mRNAs by real-time quantitative RT-PCR in three independent assays (*$P < 0.005$; **$P < 0.01$).

regulate MMP expression directly or indirectly. The Matrigel invasion assay was also performed by using HeLa cells after introduction of the *EWS-POU5F1* expression vector. Cellular invasiveness was again suppressed (Figure 4A and Table 1; $P < 0.01$), though cell migration was decreased only moderately. In addition, depletion of MMP14 protein was demonstrated by introduction of *EWS-POU5F1* into both HeLa and HCT116 colon carcinoma cells (Figure 4B). Overexpression of *EWS-POU5F1* did not affect the expression level of p27, MMP2, or MMP9 in HeLa or HCT116 cells (data not shown). These results suggest that EWS-POU5F1 suppresses cellular motility and invasion in the broad cellular context. In contrast, overexpression of $p27^{Kip1}$ did not affect either cell migration or invasion (Table 1), clearly indicating that cell motility/invasiveness is modulated in a p27-independent manner in GBS6 cells and that simple growth suppression is not sufficient to enhance the invasive activity of tumor cells.

Modulation of the Gene Expression Profile by EWS-POU5F1 *Suppression*

To investigate important downstream molecules regulated by EWS-POU5F1, alteration of global gene expression profiles by *EWS-POU5F1* knockdown was examined. We compared RNAs derived from *POU5F1*-specific siRNA-treated and control GBS6 cells (4 days after siRNA treatment) by using 54,676 probe sets of Affymetrix GeneChip Human Genome U133 Plus 2.0. We identified 98 probe sets (80 genes), the expression of which was increased more than 1.5-fold, and 55 probe sets (45 genes), the expression of which was decreased more than 1.5-fold (Figure 5A and Supplemental Table S1 at *http://ajp.amjpathol.org*). The genes whose expression was modified significantly were then classified according to gene ontology categories (Figure 5B). Interestingly,

Table 1. Invasiveness and Migration of GBS6 and HeLa Cells

	EWS-POU5F1 knockdown in GBS6		*p27* expression in GBS6		*EWS-POU5F1* expression in HeLa	
Cells and treatment	−	+	−	+	−	+
No. invasion	0.3 ± 0.4	101 ± 19*	0	0	1108 ± 85	357 ± 64*
No. migration	9.3 ± 3.2	>500*	11.1 ± 1.1	3.0 ± 0.7	3628 ± 401	1725 ± 229

Mean values ± SE of cell numbers of invasion and migration per 5×10^5 cells are exhibited.
*$P < 0.01$ versus control (−).

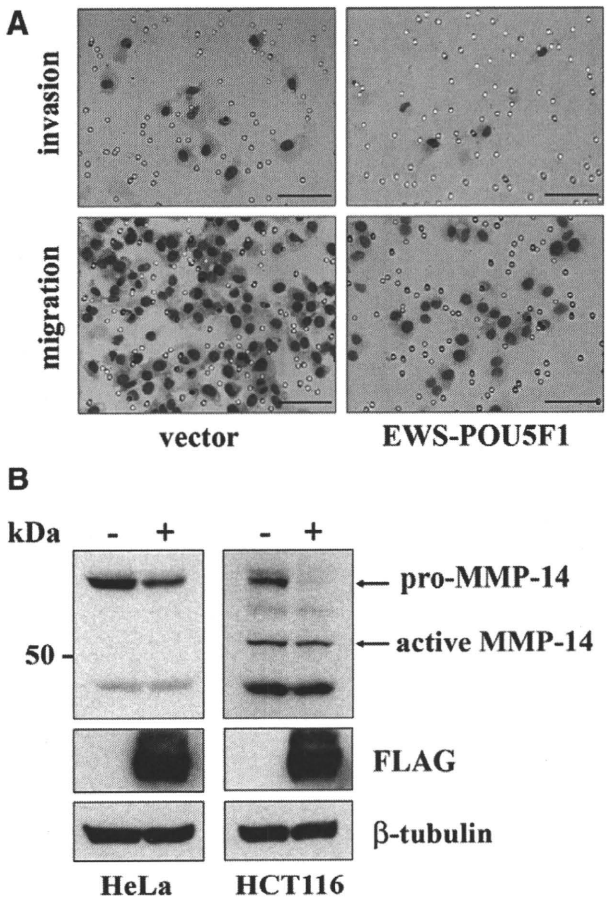

Figure 4. Inhibition of cell migration and invasion by EWS-POU5F1 in HeLa cells. **A:** Matrigel invasion assay. Giemsa-Wright staining, ×200 original magnification. Scale bars = 100 μm. **B:** Immunoblotting of HeLa cells transfected with control (−) or *EWS-POU5F1* (+) expression vectors using anti-MMP14 (**top**), anti-FLAG (**middle**), and anti-β-tubulin (**bottom**).

23.8% of up-regulated genes were involved in cell motility, invasion, or cytoskeleton, consistent with the remarkable alteration of the phenotypes in GBS6 cells. In addition, 13.3% of down-regulated and 13.8% of up-regulated genes belong to differentiation and development categories, indicating importance of the POU5F1 function in pluripotency. However, *EWS-POU5F1* knockdown did not induce GBS6 cells to differentiate toward any specific lineage.

Representative differentially expressed genes of interest belonging to motility, adhesion/invasiveness, morphology/cytoskeleton, mesodermal differentiation, and growth suppression categories are shown in Figure 5C. In motility and adhesion/invasiveness categories, up-regulation of *MMP2* was again observed, though *MT1-MMP* was up-regulated only marginally. We also noted up-regulation of *CAV1*, the mutation of which is associated with mammary carcinoma invasiveness.[22] In addition, another up-regulated gene, *F2R*, has been reported as overexpressed in human cancers with high metastatic potency.[23] Down-regulation of *ELMO1* is intriguing because it is required for promoting phagocytosis and cell shape changes.[24]

A number of genes involved in the differentiation process were up-regulated by *EWS-POU5F1* knockdown. *MGP*, *LBH*, *JUN*, *MYOF*, *CTGF*, and *MESDC2* are involved in mesodermal differentiation (Figure 5C and Supplemental Table S1 at *http://ajp.amjpathol.org*). The mesodermal origin of t(6;22) sarcoma was also supported by the fact that a number of genes encoding extracellular matrix proteins were also up-regulated. However, any specific differentiation toward muscle, bone, cartilage, or adipocytes was not supported by gene expression profiling.

Four putative tumor suppressors, *IGFBP7*, *HTRA1*, *TGFBR2*, and *SOCS3*, were up-regulated by *EWS-POU5F1* knockdown.[25–28] Although it remains unclear whether these genes are the direct targets of EWS-POU5F1, modified expression of these genes should be noted in addition to the altered state of p27, cyclin D1, and Rb. In summary, expression profiling provided important information on the molecular networks affected by the oncogenic function of EWS-POU5F1.

EWS-POU5F1 Up-Regulates the ES Cell-Specific miR302-367 Cluster

MicroRNAs (miRNAs) are noncoding RNAs consisting of approximately 22 nucleotides, which posttranscriptionally regulate mRNAs. They are important in development and differentiation, and abnormal expression of miRNAs has been reported in various neoplasms.[29,30] The miR302-367 cluster has been identified recently as ES cell-specific, and the cluster is transcriptionally regulated by Nanog, POU5F1, Sox2, and Rex1.[31,32] RT-PCR analysis revealed remarkable down-regulation of the miR302-367 cluster during knockdown of *EWS-POU5F1* (Figures 6A and 6B), suggesting that chimeric EWS-POU5F1, like wild-type POU5F1, may regulate miR302-367. The result strongly suggests that EWS-POU5F1 regulates downstream genes not only by its direct DNA binding but also through modulating the expression of miRNA.

Discussion

In the present study we show that EWS-POU5F1 enhances cellular proliferation of GBS6 sarcoma cells. Knockdown of *EWS-POU5F1* caused GBS6 cells to arrest in the G1 phase of the cell cycle. We also noted up-regulation of $p27^{Kip1}$, down-regulation of cyclin D1, and diminished phosphorylation of Rb protein. The tumor suppressor $p27^{Kip1}$ is a CDK2 inhibitor, and it inhibits the cell cycle at the G1/S transition.[33] It is likely that $p27^{Kip1}$ functions downstream from EWS-POU5F1 in oncogenic transformation. In support of this idea, exogenous introduction of $p27^{Kip1}$ blocked proliferation of GBS6 cells.

During suppression of *EWS-POU5F1*, GBS6 cells showed morphological changes similar to those seen in cellular senescence (eg, spreading of the cytoplasm, marked enlargement of cell size, and expression of senescence-associated β-galactosidase, a hallmark of senescence).[15] However, the lack of senescence-associated heterochromatin foci[16] and the reversible nature of the G1 arrest suggest that the change induced by *EWS-POU5F1* knockdown differs from senescence. Loss of $p16^{INK4A}$ might protect GBS6 cells from senescence,

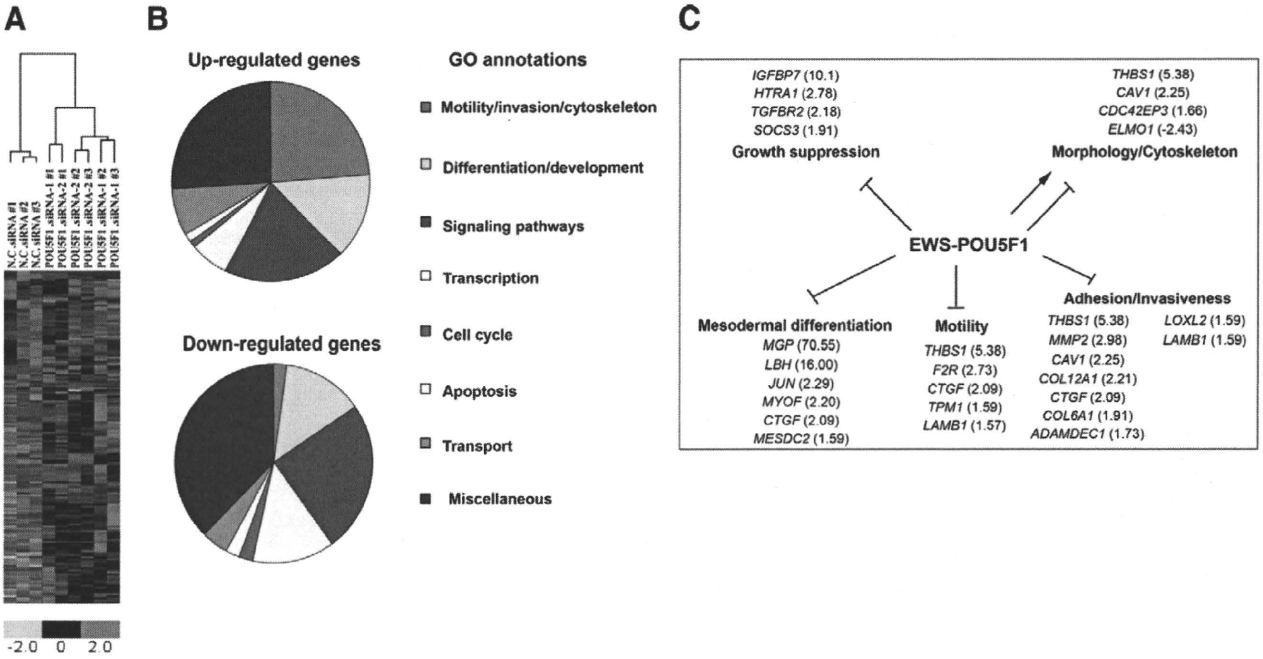

Figure 5. Gene clustering analysis across the compared populations. **A:** Heat map shows the expression of EWS-POU5F1 regulated genes in GBS6 cells treated with negative control siRNA or *POU5F1*-specific siRNAs. Up-regulated and down-regulated genes are presented in red and green, respectively. **B:** Pie charts show the distribution of the 80 up-regulated and 45 down-regulated genes in GBS6 cells transfected with *POU5F1* siRNAs according to gene ontology (GO) annotations. **C:** Prediction of the major signaling pathways affected by EWS-POU5F1. Lower bound of fold changes in each gene are indicated in parentheses.

and senescence-like morphological changes might be achieved by alteration of the actin fiber network.

The inhibitory role of EWS-POU5F1 in cell migration and invasion was unexpected. It is very likely that multiple molecular processes were responsible for increased motility and invasiveness of GBS6 cells treated with *POU5F1* siRNAs. It has been reported that RhoA activation induces actin polymerization[17] that is causatively related to cancer cell invasion and migration.[34] Paradoxical promotion of tumor invasiveness related to $p27^{Kip1}$-dependent G1 arrest has been reported in malignant melanoma with Mitf activation in which Mitf promotes melanoma proliferation by down-regulating $p27^{Kip1}$ but suppresses tumor cell invasion by the Dia1-dependent pathway.[35] Furthermore, $p27^{Kip1}$ supports cell motility through modulation of the RhoA pathway.[36] In GBS6 cells, however, introduction of $p27^{Kip1}$ affected neither cell mobility/invasiveness nor morphological changes. Those results suggest that there might be a $p27^{Kip1}$-independent pathway in RhoA activation and actin polymerization. MMP2 and MT1-MMP, which were up-regulated by knockdown of *EWS-POU5F1*, are candidate upstream regulators of RhoA because recent studies indicate these MMPs induce RhoA activation in osteosarcoma and vascular endothelial cells.[37,38] Moreover, our study indicates that increased cell motility was not a simple consequence of growth suppression. Furthermore, the present results raise an important concern for the treatment of cancer in general. That is, when treatment suppresses the expression of oncogenic transcription factors, inhibition of tumor growth might be accompanied by enhanced tumor cell invasion and metastasis.

Carcinogenesis is a multistep process that requires multiple genetic and epigenetic alterations.[39] Therefore, the fusion of *EWSR1* and *POU5F1* is not sufficient for complete carcinogenesis, and t(6;22) tumors possess additional mutations such as *p16/p14* loss. Our prelimi-

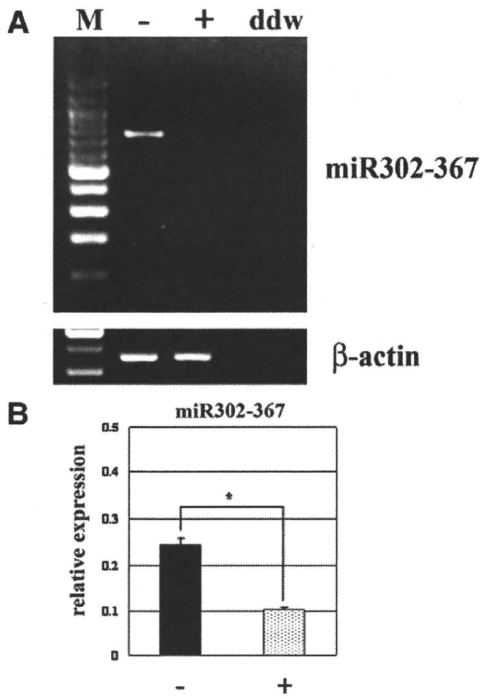

Figure 6. **A:** RT-PCR analysis of miR302-367 in GBS6 cells transfected with control (−) or POU5F1 (+). β-actin was amplified to confirm qualities and quantities of RNA. **B:** Real time quantitative RT-PCR analysis of miR302-367. Average expression was calculated in three independent experiments ($^*P < 0.005$).

nary study demonstrated that retrovirus-mediated gene transfer of *EWS-POU5F1* could immortalize but not induce full transformation of murine mesenchymal stem cells (M. Tanaka and T. Nakamura, unpublished observation). Identification of genes cooperative with *EWS-POU5F1* for carcinogenesis is important, and genetic analysis including mutagenesis experiments will provide useful information for understanding the mechanism of *POU5F1*-induced carcinogenesis. In addition, our study suggests that tumor progression toward invasive properties may be caused by genes that do not cooperate with *EWS-POU5F1* but may even counteract *EWS-POU5F1*.

It is intriguing to define important EWS-POU5F1 target genes in carcinogenesis. Because POU5F1/Oct3/4 is a transcriptional regulator, it is likely that the fusion to EWS modulates the nature of its regulatory activities for downstream target genes. Previous studies suggested that POU5F1 acquires the enhanced transcriptional activity by addition of the EWS N-terminal domain.[13,40] The target genes for POU5F1 have been extensively investigated by using ES cells.[4,41,42] In these studies POU5F1 is found associated with SOX2 and/or Nanog, both of which are also expressed in GBS6 cells (data not shown). However, the down-regulated genes in *EWS-POU5F1* knockdown GBS6 cells did not always overlap with POU5F1 target genes in ES cells, probably because of the different cellular context between ES cells and sarcoma cells. Alternatively, the addition of the EWS N-terminal domain may alter the binding specificity of POU5F1 to the target sequences. Nevertheless, it is still possible that there are common target genes for both EWS-POU5F1 and wild-type POU5F1. In a comparison between genes showing altered expression on *EWS-POU5F1* knockdown in the present study and the genes detected in chromatin immunoprecipitation (ChIP)-on-chip or chromatin immunoprecipitation-paired-end ditag (ChIP-PET) studies,[41,42] *INSIG1*, *EPHA4*, *DHCR7*, *ANKS1B*, *ANO4*, *RDH10*, *PHF19*, *BNIP3*, and *TRIB1* are good candidates for common target genes of POU5F1 or EWS-POU5F1 in organogenesis or sarcomagenesis. In addition, the miR302-367 cluster has been identified as a target of ES cell-associated transcription factors, including POU5F1.[32] Down-regulation of miR302-367 on *EWS-POU5F1* knockdown strongly suggests that EWS-POU5F1 regulates gene expression by recognition of a target sequence as well as miRNA-mediated mRNA inhibition. In fact, overexpression of miR302 induces cell cycle progression of ES cells.[43] Interestingly, miR302 represses protein expression of cyclin D1 in ES cells, the opposite effect for EWS-POU5F1 in GBS6 cells, suggesting cell context-dependent function of the miR302-467 cluster. Further studies are needed to identify key downstream molecules controlling cell proliferation and/or cell motility and invasiveness.

Acknowledgments

We thank Dr. Kei-ichi Nakayama for providing a human p27 expression vector, Dr. Eiji Hara and Dr. Akiko Takahashi for valuable discussion, and Ms. Sayuri Amino-Shibuya and Ms. Rie Furuya for technical assistance.

References

1. Schöler HR, Dressler GR, Balling R, Rohdewohld H, Gruss P: Oct-4: a germline-specific transcription factor mapping to the mouse t-complex. EMBO J 1990, 9:2185–2195
2. Nichols J, Zevnik B, Anastassiadis K, Niwa H, Klewe-Nebenius D, Chambers I, Schöler H, Smith A: Formation of pluripotent stem cells in the mammalian embryo depends on the POU transcription factor Oct4. Cell 1998, 95:379–391
3. Niwa H, Miyazaki J, Smith AG: Quantitative expression of Oct-3/4 defines differentiation, dedifferentiation or self-renewal of ES cells. Nat Genet 2000, 24:372–376
4. Matoba R, Niwa H, Masui S, Ohtsuka S, Carter MG, Sharov AA, Ko MS: Dissecting Oct3/4-regulated gene networks in embryonic stem cells by expression profiling. PLoS ONE 2006, 1:e26
5. Ivanova N, Dobrin R, Lu R, Kotenko I, Levorse J, DeCoste C, Schafer X, Lun Y, Lemischka IR: Dissecting self-renewal in stem cells with RNA interference. Nature 2006, 442:533–538
6. Takahashi K, Yamanaka S: Induction of pluripotent stem cells from mouse embryonic and adult fibroblast cultures by defined factors. Cell 2006, 126:1–14
7. Kim JB, Zaehres H, Wu G, Gentile L, Ko K, Sebastiano V, Araúzo-Bravo MJ, Ruau D, Han DW, Zenke M, Schöler HR: Pluripotent stem cells induced from adult neural stem cells by reprogramming with two factors. Nature 2008, 454:646–650
8. Jin T, Branch DR, Zhang X, Qi S, Youngson B, Goss PE: Examination of POU homeobox genes in breast cancer cells. Int J Cancer 1999, 81:104–112
9. Gidekel S, Pizov G, Bergman Y, Pikarsky E: Oct3/4 is a dose-dependent oncogenic fate determinant. Cancer Cell 2003, 4:361–370
10. Looijenga LH, Stoop H, de Leeuw HP, de Gouveia Brazao CA, Gillis AJ, van Roozendaal KE, van Zoelen EJ, Weber RF, Wolffenbuttel KP, van Dekken H, Honecker F, Bokemeyer C, Perlman EJ, Schneider DT, Kononen J, Sauter G, Oosterhuis JW: POU5F1 (OCT3/4) identifies cells with pluripotent potential in human germ cell tumors. Cancer Res 2003, 63:2244–2250
11. Atlasi Y, Mowla SJ, Ziaee SA, Bahrami AR: OCT-4, an embryonic stem cell marker, is highly expressed in bladder cancer. Int J Cancer 2007, 120:1598–1602
12. Yamaguchi S, Yamazaki Y, Ishikawa Y, Kawaguchi N, Mukai H, Nakamura T: EWSR1 is fused to POU5F1 in a bone tumor with translocation t(6;22)(p21;q12). Genes Chromosomes Cancer 2005, 43:217–222
13. Möller E, Stenman G, Mandahl N, Hamberg H, Mölne L, van den Oord JJ, Brosjö O, Mertens F, Panagopoulos I: POU5F1, encoding a key regulator of stem cell pluripotency, is fused to EWSR1 in hidradenoma of the skin and mucoepidermoid carcinoma of the salivary glands. J Pathol 2008, 215:78–86
14. Kawamura-Saito M, Yamazaki Y, Kaneko K, Kawaguchi N, Kanda H, Mukai H, Gotoh T, Motoi T, Fukayama M, Aburatani H, Takizawa T, Nakamura T: Fusion between CIC and DUX4 up-regulates PEA3 family genes in Ewing-like sarcomas with t(4;19)(q35;q13) translocation. Hum Mol Genet 2006, 15:2125–2137
15. Lundberg AS, Hahn WC, Gupta P, Weinberg RA: Genes involved in senescence and immortalization. Curr Opin Cell Biol 2000, 12:705–709
16. Narita M, Nũnez S, Heard E, Narita M, Lin AW, Hearn SA, Spector DL, Hannon GJ, Lowe SW: Rb-mediated heterochromatin formation and silencing of E2F target genes during cellular senescence. Cell 2003, 113:703–716
17. Ridley AJ, Hall A: The small GTP-binding protein rho regulates the assembly of Focal adhesions and actin stress fibers in response to growth factors. Cell 1992, 70:401–410
18. Hanahan D, Weinberg RA: The hallmarks of cancer. Cell 2000, 100:57–70
19. Seiki M: The cell surface: the stage for matrix metalloproteinase regulation of migration. Curr Opin Cell Biol 2002, 14:624–635
20. Seiki M, Mori H, Kajita M, Uekita T, Itoh Y: Membrane-type 1 matrix metalloproteinase and cell migration. Biochem Soc Symp 2003, 70:253–262
21. Seiki M, Koshikawa N, Yana I: Role of pericellular proteolysis by membrane-type 1 matrix metalloproteinase in cancer invasion and angiogenesis. Cancer Metastasis Rev 2003, 22:129–143
22. Bonuccelli G, Casimiro MC, Sotgia F, Wang C, Liu M, Katiyar S, Zhou J, Dew E, Capozza F, Daumer KM, Minetti C, Milliman JN, Alpy F, Rio MC,

Tomasetto C, Mercier I, Flomenberg N, Frank PG, Pestell RG, Lisanti MP: Caveolin-1 (P132L), a common breast cancer mutation, confers mammary cell invasiveness and defines a novel stem cell/metastasis-associated gene signature. Am J Pathol 2009, 174:1650–1662
23. Boire A, Covic L, Agarwal A, Jacques S, Sherifi S, Kuliopulos A: PAR1 is a matrix metalloprotease-1 receptor that promotes invasion and tumorigenesis of breast cancer cells. Cell 2005, 120:303–313
24. Gumienny TL, Brugnera E, Tosello-Trampont AC, Kinchen JM, Haney LB, Nishiwaki K, Walk SF, Nemergut ME, Macara IG, Francis R, Schedl T, Qin Y, Van Aelst L, Hengartner MO, Ravichandran KS: CED-12/ELMO, a novel member of the CrkII/Dock180/Rac pathway, is required for phagocytosis and cell migration. Cell 2001, 107:27–41
25. Wilson EM, Oh Y, Hwa V, Rosenfeld RG: Interaction of IGF-binding protein-related protein 1 with a novel protein, neuroendocrine differentiation factor, results in neuroendocrine differentiation of prostate cancer cells. J Clin Endocr Metab 2001, 86:4504–4511
26. Chien J, Staub J, Hu SI, Erickson-Johnson MR, Couch FJ, Smith DI, Crowl RM, Kaufmann SH, Shridhar V: A candidate tumor suppressor HtrA1 is downregulated in ovarian cancer. Oncogene 2004, 23:1636–1644
27. Markowitz S, Wang J, Myeroff L, Parsons R, Sun L, Lutterbaugh J, Fan RS, Zbrowska E, Kinzler KW, Vogelstein B, Brattain M, Willson JKV: Inactivation of the type II TGF-beta receptor in colon cancer cell with microsatellite instability. Science 1995, 268:1336–1338
28. He B, You L, Uematsu K, Zang K, Xu Z, Lee AY, Costello JF, McCormick F, Jablons DM: SOCS-3 is frequently silenced by hypermethylation and suppresses cell growth in human lung cancer. Proc Natl Acad Sci USA 2003, 100:14133–14138
29. Lagos-Quintana M, Rauhut R, Yalcin A, Meyer J, Lendeckel W, Tuschl T: Identification of tissue-specific microRNAs from mouse. Curr Biol 2002, 12:735–739
30. Aravin AA, Lagos-Quintana M, Yalcin A, Zavolan M, Marks D, Snyder B, Gaasterland T, Meyer J, Tuschl T: The small RNA profile during Drosophila melanogaster development. Dev Cell 2003, 5:337–350
31. Suh MR, Lee Y, Kim JY, Kim SK, Moon SH, Lee JY, Cha KY, Chung HM, Yoon HS, Moon SY, Kim VN, Kim KS: Human embryonic stem cells express a unique set of microRNAs. Dev Biol 2004, 270:488–498
32. Barroso-del Jesus A, Romero-López C, Lucena-Aguilar G, Melen GJ, Sanchez L, Ligero G, Berzal-Herranz A, Menendez P: Embryonic stem cell-specific miR302-367 cluster: human gene structure and functional characterization of its core promoter. Mol Cell Biol 2008, 28:6609–6619
33. Sherr CD, Roberts JM: CDK inhibitors: positive and negative regulators of G1-phase progression. Genes Dev 2001, 13:1501–1512
34. Yamaguchi H, Condeelis J: Regulation of the actin cytoskeleton in cancer cell migration and invasion. Biochim Biophys Acta 2007, 1773:642–652
35. Carreira S, Goodall J, Denat L, Rodriguez M, Nuciforo P, Hoek KS, Testori A, Larue L, Goding CR: Mitf regulation of Dia1 controls melanoma proliferation and invasiveness. Genes Dev 2006, 20:3426–3439
36. Fromique O, Hamidouche Z, Marie PJ: Nlockade of the RhoA-JNK-c-Jun-MMP2 cascade by atorvastatin reduces osteosarcoma cell invasion. J Biol Chem 2008, 283:30549–30556
37. Sugimoto K, Ishibashi T, Sawamura T, Inoue N, Kamioka M, Uekita H, Ohkawara H, Sakamoto T, Sakamoto N, Okamoto Y, Takuwa Y, Kakino A, Fujita Y, Tanaka T, Teramoto T, Maruyama Y, Takeishi Y: LOX-1-MT1-MMP axis is crucial for RhoA and Rac1 activation induced by oxidized low-density lipoprotein in endothelial cells. Cardiovasc Res 2009, 84:127–136
38. Besson A, Gurian-West M, Schmidt A, Hall A, Roberts JM: p27Kip1 modulates cell migration through the regulation of RhoA activation. Genes Dev 2004, 18:862–876
39. Weinberg RA: Multistep tumorigenesis: the biology of cancer. Edited by RA Weinberg. Garland Science, New York, NY 2007, pp 399–462
40. Lee J, Kim JY, Kang IY, Kim HK, Han YM, Kim J: The EWS-Oct-4 fusion gene encodes a transforming gene. Biochem J 2007, 406:519–526
41. Boyer LA, Lee TI, Cole MF, Johnstone SE, Levine SS, Zucker JP, Guenther MG, Kumar RM, Murray HL, Jenner RG, Gifford DK, Melton DA, Jaenisch R, Young RA: Core transcriptional regulatory circuitry in human embryonic stem cells. Cell 2005, 122:947–956
42. Loh YH, Wu Q, Chew JL, Vega VB, Zhang W, Chen X, Bourque G, George J, Leong B, Liu J, Wong KY, Sung KW, Lee CW, Zhao XD, Chiu KP, Lipovich L, Kuznetsov VA, Robson P, Stanton LW, Wei CL, Ruan Y, Lim B, Ng HH: The Oct4 and Nanog transcription network regulates pluripotency in mouse embryonic stem cells. Nat Genet 2006, 38:431–440
43. Greer Card DA, Hebbar PB, Li L, Trotter KW, Komatsu Y, Mishina Y, Archer TK: Oct4/Sox2-regulated miR-302 targets cyclin D1 in human embryonic stem cells. Mol Cell Biol 2008, 28:6426–6438

Tiss. Cult. Res. Commun. 28: 109–000 (2009)

遺伝子導入技術を利用した幹細胞の分化誘導法

田代　克久[1)]、稲村　　充[1,2)]、川端　健二[1,3)]、水口　裕之[1,2)]

[1)] 独立行政法人　医薬基盤研究所　遺伝子導入制御プロジェクト
[2)] 大阪大学大学院薬学研究科　分子生物学分野
[3)] 大阪大学大学院薬学研究科　医薬基盤科学分野

要約　　多分化能及び自己複製能を有している胚性幹（ES）細胞や人工多能性幹（iPS）細胞を医療へ応用するには、両細胞を目的の細胞に選択的に分化誘導する技術の確立が必須である。そこで我々は、アデノウイルス（Ad）ベクターを用いた分化関連遺伝子の導入による分化誘導法の確立を試みた。マウス ES、iPS 細胞への効率的な遺伝子導入法の確立を行ったところ、CMV エンハンサーと β–アクチンプロモーターのハイブリッドプロモーターである CA プロモーターを有する Ad ベクターが高効率遺伝子導入に適していた。そこでこのベクターを用いて、脂肪細胞または骨芽細胞への分化に必須の PPARγ 遺伝子、Runx2 遺伝子をマウス ES 細胞、iPS 細胞に導入したところ、液性因子のみを使用する従来の分化誘導法と比較し、極めて効率良く脂肪細胞、骨芽細胞へ分化させることに成功した。このように Ad ベクターを用いた遺伝子導入技術は幹細胞の分化制御に有用であり、今後、医療への応用等が期待される。

キーワード：　幹細胞、分化誘導、遺伝子導入、アデノウイルスベクター

【序　　文】

幹細胞は多分化能と自己複製能という二つの特異な性質を有している細胞であり、この幹細胞の性質を利用し、損傷した細胞・組織を人工的に再生させ、医療へ応用することが再生医療とよばれている。再生医療への応用が期待されている幹細胞は、受精卵（胚）から樹立された胚性幹（ES）細胞[1,2)]や、骨髄や脂肪組織などに存在する体性幹細胞[3)]、そして近年体細胞から樹立された人工多能性幹（iPS）細胞[4,5)]である。これらの幹細胞を医療へ応用するには、幹細胞を特定の細胞（治療用細胞）へ選択的に分化させる技術の確立が必須である。これまでは主にサイトカインや増殖因子等の液性因子単独による分化誘導法が実施されてきたが、その分化効率には問題点が残されていた。細胞分化は種々の遺伝子の活性化および抑制化により誘導されるため、分化関連遺伝子の発現量を人工的に操作することにより、幹細胞の分化を制御できると考えられる。そこで、我々のグループは幹細胞へ分化関連遺伝子を効率良く導入するこ

連絡者：水口裕之
大阪大学大学院薬学研究科　分子生物学分野
〒565–0871　大阪府吹田市山田丘1–6
TEL：06–6879–8185、FAX：06–6879–8185
E-mai：mizuguch@phs.osaka-u.ac.jp

とにより、高純度の治療用細胞を大量に作製することを目的として研究を進めてきた[6,7,8]。今回、アデノウイルス（Ad）ベクターを用いてマウス ES 細胞、マウス iPS 細胞（京都大学 山中伸弥教授より供与）への高効率遺伝子導入法の確立および脂肪細胞・骨芽細胞への分化誘導法の確立を行った[9] ので、これについて概説する。

1．未分化マウス ES、iPS 細胞への遺伝子導入

これまでマウス ES 細胞に対しては、エレクトロポレーション法やレトロウイルスベクター、レンチウイルスベクターなどが外来遺伝子の導入法として汎用されてきた[10,11,12,13,14]。しかしこれらの方法では、導入遺伝子がランダムに染色体に組み込

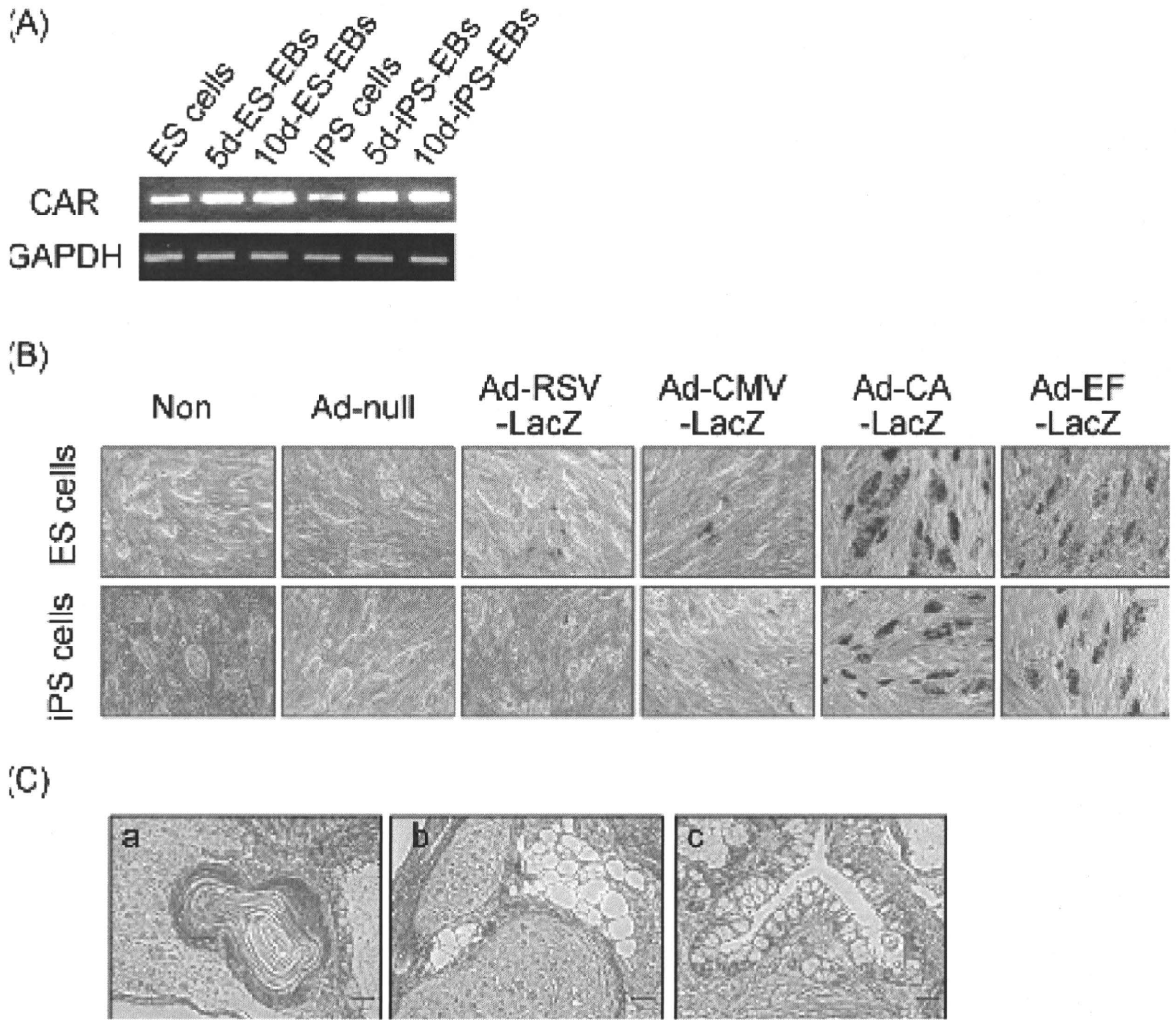

図 1　Ad ベクターによるマウス ES、iPS 細胞への遺伝子導入
（A）マウス ES、iPS 細胞およびマウス ES 細胞由来胚様体（ES-EB）、iPS 細胞由来胚様体（iPS-EB）における CAR の発現。5d：5 日間培養。10d：10日間培養　（B）各種 LacZ 発現 Ad ベクターを用いてマウス ES、iPS 細胞へ遺伝子導入して24時間後の X-gal 染色像。Ad-null：外来遺伝子を搭載していない Ad ベクター。Scale bar, 60 μm　（C）Ad ベクターを作用させたマウス iPS 細胞由来奇形腫の HE 染色像。a, 外胚葉（表皮組織）b, 中胚葉（軟骨組織、脂肪組織）c, 内胚葉（腸管上皮組織）Scale bar, 30 μm（Stem Cells, 27, 1802–1811, 2009.　Figure 1A, 2A, 2E より一部改変）

まれるだけでなく、細胞分化後も遺伝子発現が続き、細胞機能に影響を及ぼす可能性があることが問題となる。医療への応用を考慮すると、一定の時期にのみ幹細胞に導入遺伝子を発現させて目的細胞へ分化させ、細胞分化完了後は導入遺伝子の発現が消失することが好ましい。すなわち、ES 細胞や iPS 細胞を含む幹細胞の分化誘導には、導入遺伝子を一過性に効率良く発現させるベクターが望まれる。

アデノウイルス（Ad）ベクターは既存の遺伝子導入ベクターの中で最も高い遺伝子発現効率を示すことや非分裂細胞にも遺伝子導入可能であることから、基礎研究だけでなく遺伝子治療臨床研究にも広く使用されている。特に、Ad ベクターを用いて導入した遺伝子は一過性に発現し、宿主染色体への組み込みは伴わないため、Ad ベクターは幹細胞の分化誘導系に適していると考えられる。そこで著者らは、まず Ad ベクターを用いてマウス ES 細胞、iPS 細胞への遺伝子導入法の確立を行った。Ad ベクターは細胞表面上の受容体 CAR（coxsackievirus and adenovirus receptor）を介して感染する[15,16]。マウス ES、iPS 細胞における CAR の発現を検討したところ、両細胞は CAR を発現していることが明らかとなり（図 1A）[6,8]、Ad ベクターにより遺伝子導入可能であることが示唆された。次にプロモーターの異なる 4 種類（RSV、CMV、CA（βアクチンプロモーターと CMV エンハンサーからなるハイブリッドプロモーター）、EF-1α）の β-galactosidase（LacZ）発現 Ad ベクターを調製した。マウス ES 細胞、iPS 細胞へ各種 Ad ベクターを 3,000 vector particles（VP）/cell の濃度で作用させて LacZ 発現を解析したところ、従来の遺伝子導入実験で汎用されている RSV プロモーターや CMV プロモーターではほとんど機能せず、CA および EF-1α プロモーターを有する Ad ベクターを用いることにより極めて効率良く遺伝子導入できることが明らかとなった（図 1B）。

次に Ad ベクターによる遺伝子導入がマウス iPS 細胞の多分化能に影響を与えるかどうかを検討した。CA プロモーターを有する Ad ベクターにより遺伝子導入したマウス iPS 細胞を免疫不全マウスに皮下注射し、形成させた奇形腫を解析した。その結果、Ad ベクターを作用させて形成した奇形腫は、皮膚（外胚葉）、軟骨（中胚葉）および消化管様構造（内胚葉）などを含んでいたことから、多能性を保持していることが確認された（図 1C）。なお、マウス ES 細胞においても同様の結果が得られた。したがって、Ad ベクターはマウス ES、iPS 細胞の多分化能を保持させたまま効率良く外来遺伝子を導入可能なベクターであることが示された。

2．マウス ES 細胞由来胚様体、iPS 細胞由来胚様体への遺伝子導入

マウス ES 細胞から目的の細胞へ分化させる場合、まず、胚様体（EB）とよばれる発生の初期胚に似た構造を有する細胞集合体を形成させ、その後液性因子などを加えることにより目的の細胞に分化させるという手法が一般的である。マウス ES 細胞由来 EB（ES-EB）、iPS 細胞由来 EB（iPS-EB）も CAR を発現していた（図 1A）ことから、Ad ベクターによる遺伝子導入が可能であると考えられた。そこで上述の LacZ 発現 Ad ベクターを用いて ES-EB、iPS-EB への遺伝子導入効率を評価した。その結果、ES-EB および iPS-EB において CA プロモーターを有する Ad ベクターを作用させた場合に最も高い LacZ 発現が観察された（図 2A）。興味深いことに、CMV プロモーターはマウス ES 細胞や ES-EB、マウス iPS 細胞において活性が低いにも関わらず、iPS-EB においては比較的高い遺伝子発現を示した（図 2A）。これらの結果から、マウス ES 細胞や iPS 細胞だけでなく、ES-EB および iPS-EB においても効率の良い遺伝子発現にはプロモーターの選択が重要であることが示され、マウス ES 細胞、iPS 細胞そしてこれら由来の EB

への遺伝子導入にはCAプロモーターが有効であることが明らかとなった。

ES、iPS細胞から目的細胞への効率的な分化誘導にはEB内部においても外来遺伝子を発現させることが重要であると考えられる。そこで次にAdベクターにより導入した外来遺伝子がEBの内部でも発現しているかどうか、共焦点レーザー顕微鏡にて解析した。赤色蛍光蛋白質であるmCherryを発現するAdベクター、Ad-CA-mCherryを作製し、5日間培養して作製したES-EBおよびiPS-EBへ遺伝子導入した。その結果、mCherryの発現はEB周縁部でしか観察されなかった（図2B,

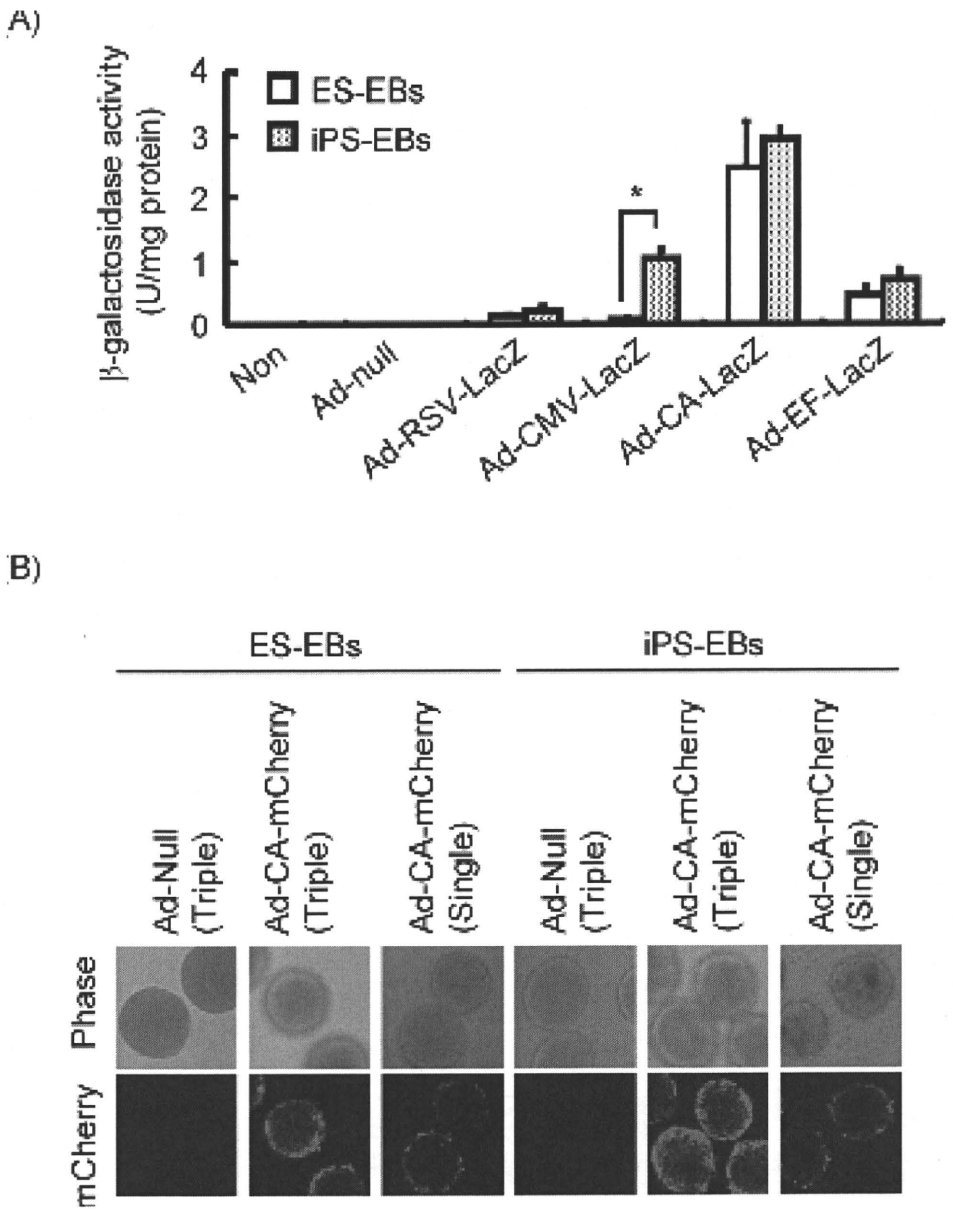

図2　Adベクターによるマウス ES 細胞由来胚様体、iPS 細胞由来胚様体への遺伝子導入
（A）各種 LacZ 発現 Ad ベクターを ES 細胞由来 EB、iPS 細胞由来EBへ遺伝子導入して48時間後の β–ガラクトシダーゼ活性。* $p < 0.01$ Scale bar, 60 μm　（B）Day 5 のみ（Single）、または Day 0, 2, 5（Triple）で ES-EB または iPS-EB へ Ad-CA-mCherry を作用させて 2 日後の共焦点レーザー顕微鏡像（Stem Cells, 27, 1802–1811, 2009.　Figure 3B, 3C より一部改変）

Single)。これは、EB を構成する細胞が物理的な障害となるために Ad ベクターが EB の内部に到達できないことが原因であると推測された。そこで、Ad ベクターによる遺伝子導入を複数回行うことを試みた。浮遊培養中の ES、iPS 細胞に Ad ベクターによる遺伝子導入を行い（Day 0)、2 日間培養した。そして 2 日目（day 2）と 5 日目（day 5）の EB に再度 Ad ベクターで遺伝子導入を行った。つまり、0、2、5 日目の合計 3 回 Ad ベクターによる遺伝子導入を行った（triple transduction)。その結果、ES-EB、iPS-EB の内部においても mCherry の発現が観察された（図 2B)。以上の結果より、EB の内部で外来遺伝子を発現させるには Ad ベクターの複数回作用が有効であることが示された。

3．脂肪細胞、骨芽細胞への分化誘導

Ad ベクターを用いた遺伝子導入技術が分化誘導系に応用できるかどうかを検討するため、マウス ES 細胞、iPS 細胞へ機能遺伝子を導入することを試みた。ES、iPS 細胞からの分化モデルとして脂

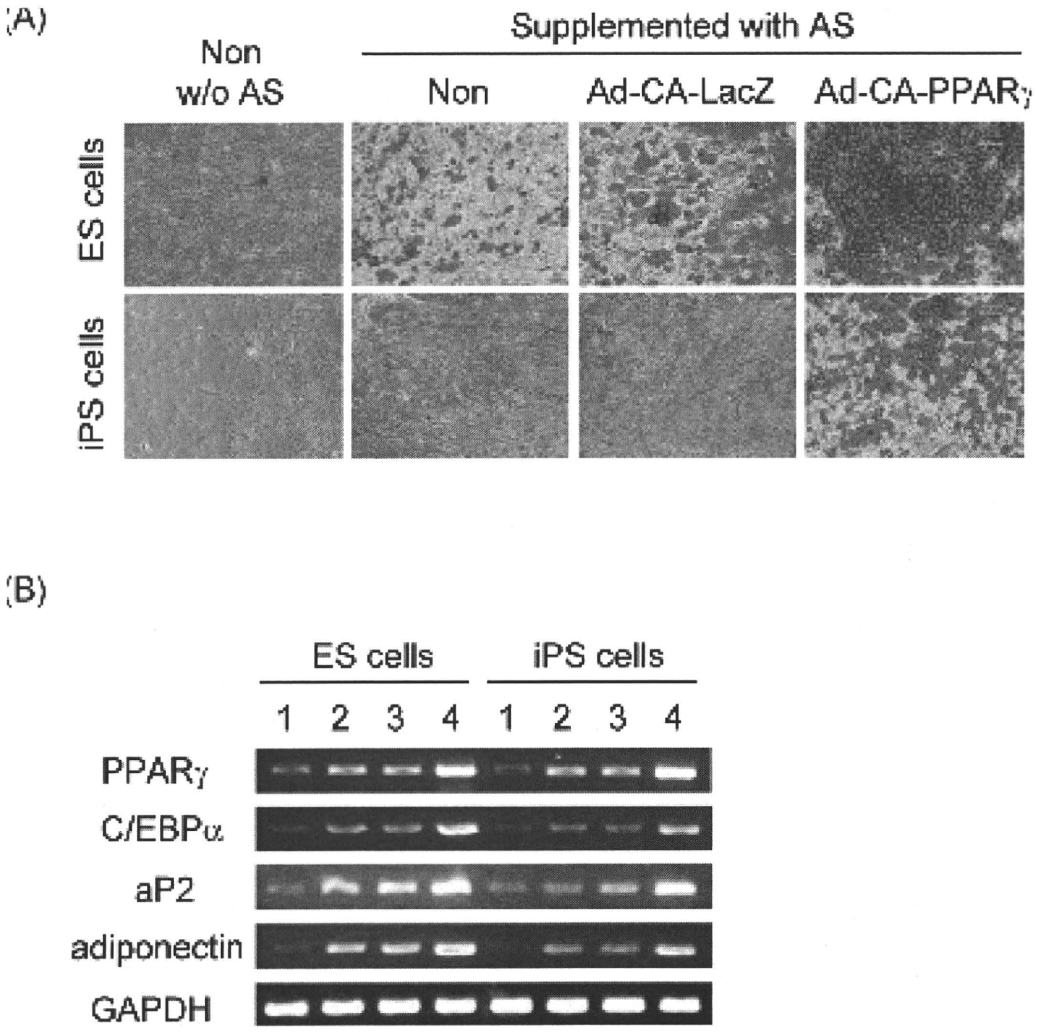

図 3　ES、iPS 細胞の脂肪細胞分化の評価
(A) ES、iPS 細胞由来分化細胞のオイルレッド O 染色像。AS：Adipogenic Supplements, w/o: without. Scale bar, 60 μm　(B) ES、iPS 細胞由来分化細胞における脂肪細胞特異的なマーカー遺伝子の発現。1、液性因子無添加　2、液性因子添加　3、液性因子添加 +Ad-CA-LacZ 作用　4、液性因子添加 +Ad-CA-PPARγ 作用（Stem Cells, 27, 1802–1811, 2009.　Figure 4A, 4C より一部改変）

肪細胞への分化誘導を行うとともに、脂肪細胞分化に必須の遺伝子である PPARγ（peroxisome proliferator-activated receptor gamma）遺伝子[17,18]をES、iPS 細胞へ導入することにより、脂肪細胞への分化効率が上昇するかどうかを検討した。上記の Triple Transduction 法を用いて両細胞へ LacZ 遺伝子（コントロール）または PPARγ 遺伝子を導入し、脂肪細胞分化用の液性因子（インスリン、デキサメタゾンなど）を含む培地中で15日間接着培養した。オイルレッド O 染色により脂肪細胞への分化効率を評価した結果、iPS 細胞の脂肪細胞への分化効率は ES 細胞の分化効率よりも低いものの、液性因子を作用させて培養することにより両細胞とも脂肪滴が観察された（図 3A, b, f）。さらに、液性因子のみを用いた分化誘導法と比較し、液性因子を加えさらに Ad ベクターによる PPARγ 遺伝子を導入した ES 細胞および iPS 細胞は、極めて効率良く脂肪細胞へ分化していることも示された

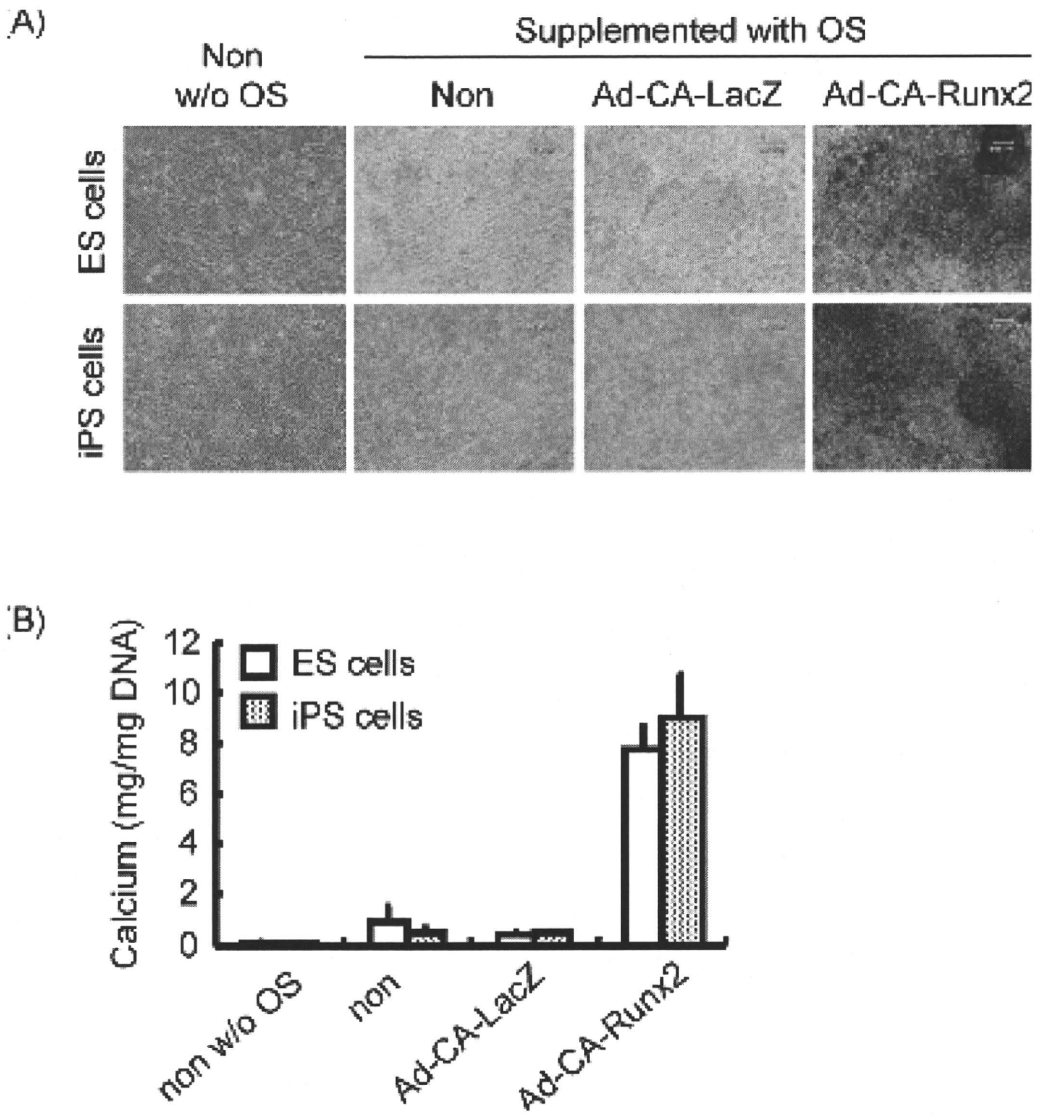

図 4　ES、iPS 細胞の骨芽細胞分化の評価
（A）ES、iPS 細胞由来分化細胞の von Kossa 染色像。OS：Osteogenic Supplements, w/o: without. Scale bar, 60 μm　（B）ES、iPS 細胞由来分化細胞の石灰化（カルシウム）の定量。（Stem Cells, 27, 1802–1811, 2009.　Figure 5B, 5C より一部改変）

(図 3A, d, h)。すなわち、従来の方法では ES 細胞において約50％の細胞が、iPS 細胞において20－30％の細胞がそれぞれオイルレッド O で染色されたのに対し、PPARγ遺伝子を導入した ES、iPS 細胞においては80－90％の細胞がオイルレッド O に染色された。また、Ad ベクターを用いた PPARγ遺伝子導入による脂肪細胞への分化効率の上昇は、脂肪細胞特異的なマーカー遺伝子の発現上昇によっても確認された（図 3B)。なお、LacZ 遺伝子を導入した細胞ではこのような分化効率の上昇はみとめられなかった。これらの結果から、マウス ES 細胞、iPS 細胞の脂肪細胞への分化効率は Ad ベクターを用いた PPARγ遺伝子の導入により改善できることが示された。

次に、Ad ベクターによる遺伝子導入がその他の細胞種への分化誘導系にも有用であるかどうかを検討するため、マウス ES 細胞、iPS 細胞から骨芽細胞への分化誘導を試みた。今回の分化誘導系においては骨芽細胞分化のマスター遺伝子である Runx2（runt-related transcription factor 2）遺伝子[19,20] を Ad ベクターにより発現させた。Ad-CA-Runx2 を EB へ 3 回作用させ、骨芽細胞分化用の液性因子（βグリセロリン酸、アスコルビン酸など）中で接着培養した。骨芽細胞は多量の骨基質蛋白質（I 型コラーゲン等）を生成・分泌し、そして石灰化を起こすことで骨組織を構築する細胞である[21]。そこでマウス ES、iPS 細胞由来の細胞が石灰化を生ずる骨芽細胞へ分化しているかどうかを von Kossa 染色により解析した。その結果、液性因子を作用させることにより石灰化が検出されたものの、その分化効率は低く、20％以下の細胞しか石灰化を起こしていなかった（図 4A, b, f)。一方、Runx2 遺伝子を導入した ES、iPS 細胞は、液性因子のみで培養した細胞、および LacZ 遺伝子を導入した細胞と比較し、石灰化した細胞が著明に増加していること明らかとなった（図 4A, d, h)。また、沈着した石灰化を定量化したところ、LacZ 遺伝子導入群においては液性因子のみの誘導法と著差は認められなかったものの、Runx2 遺伝子導入細胞においては約 8 倍、石灰化が上昇していた（図 4B)。これらの結果から、Ad ベクターによる Runx2 遺伝子の導入によりマウス ES、iPS 細胞から骨芽細胞へ効率良く分化誘導可能であることが示された。このように最適化した Ad ベクターを用いたマウス ES、iPS 細胞への分化関連遺伝子の導入により、脂肪細胞および骨芽細胞への分化効率を飛躍的に改善できることが示され、本遺伝子導入技術はマウス ES、iPS 細胞を用いた細胞分化研究に有用であると考えられた。

おわりに

これまでにもレトロウイルスベクターなどの恒常的遺伝子発現系を用いて ES 細胞から標的の細胞への分化誘導は行われてきた。しかし、これらの手法では機能遺伝子が染色体に挿入されるため治療用に適しておらず、一過性の遺伝子導入系の分化誘導が望まれていた。今回、著者らは Ad ベクターを用いたマウス ES、iPS 細胞への高効率遺伝子導入法の確立に成功し、さらにその遺伝子導入技術を利用して分化関連遺伝子をマウス ES、iPS 細胞へ導入することにより特定の細胞へ効率良く分化誘導することに成功した。なお、異なる iPS 細胞株についても今回と同様の結果が得られており[9]、幅広い ES、iPS 細胞株に適用可能であることが示唆されている。また、今回は示していないが、分化が完了した細胞では Ad ベクター由来の遺伝子発現はほとんどみとめられないことも確認している[8]。したがって、Ad ベクターは幹細胞を用いた分化誘導研究において、効率面だけでなく安全面においても非常に有用であると考えられる。現在、著者らのグループでは Ad ベクターを用いた遺伝子導入技術がその他の細胞種への分化誘導系へ応用可能かどうか、マウスおよびヒトの ES、iPS

細胞を用いて検討中である。また、著者らは Ad ベクターを用いて間葉系幹細胞、ヒト造血幹細胞への高効率遺伝子導入法も確立しており[7,22,23,24]、これらの細胞を用いて医療応用を目指した研究を進めている。一過性発現を示す Ad ベクターを用いた遺伝子導入技術は、幹細胞研究・再生医療研究において重要なツールになるものと考えられ、今後の益々の応用が期待される。

文　　献

1) Evans M. J., Kaufman M. H.: Establishment in culture of pluripotential cells from mouse embryos. Nature, 292, 154–156, 1981.
2) Thomson J. A., Itskovitz-Eldor J., Shapiro S. S., Waknitz M. A., Swiergiel J. J., Marshall V. S., Jones J. M.: Embryonic stem cell lines derived from human blastocysts. Science, 282, 1145–1147, 1998.
3) Pittenger M. F., Mackay A. M., Beck S. C., Jaiswal R. K., Douglas R., Mosca J. D., Moorman M. A., Simonetti D. W., Craig S., Marshak D. R.: Multilineage potential of adult human mesenchymal stem cells. Science, 284, 143–147, 1999.
4) Takahashi K., Yamanaka S.: Induction of pluripotent stem cells from mouse embryonic and adult fibroblast cultures by defined factors. Cell, 126, 663–676, 2006.
5) Takahashi K., Tanabe K., Ohnuki M., Narita M., Ichisaka T., Tomoda K., Yamanaka S.: Induction of pluripotent stem cells from adult human fibroblasts by defined factors. Cell, 131, 861–872, 2007.
6) Kawabata K., Sakurai F., Yamaguchi T., Hayakawa T., Mizuguchi H.: Efficient gene transfer into mouse embryonic stem cells with adenovirus vectors. Mol Ther, 12, 547–554, 2005.
7) Mizuguchi H., Sasaki T., Kawabata K., Sakurai F., Hayakawa T.: Fiber-modified adenovirus vectors mediate efficient gene transfer into undifferentiated and adipogenic-differentiated human mesenchymal stem cells. Biochem Biophys Res Commun, 332, 1101–1106, 2005.
8) Tashiro K., Kawabata K., Sakurai H., Kurachi S., Sakurai F., Yamanishi K., Mizuguchi H.: Efficient adenovirus vector-mediated PPAR gamma gene transfer into mouse embryoid bodies promotes adipocyte differentiation. J Gene Med, 10, 498–507, 2008.
9) Tashiro K., Inamura M., Kawabata K., Sakurai F., Yamanishi K., Hayakawa T., Mizuguchi H.: Efficient adipocyte and osteoblast differentiation from mouse induced pluripotent stem cells by adenoviral transduction. Stem Cells, 27, 1802–1811, 2009.
10) Cherry S. R., Biniszkiewicz D., van Parijs L., Baltimore D., Jaenisch R.: Retroviral expression in embryonic stem cells and hematopoietic stem cells. Mol Cell Biol, 20, 7419–7426, 2000.
11) Kyba M., Perlingeiro R. C., Daley G. Q.: HoxB4 confers definitive lymphoid-myeloid engraftment potential on embryonic stem cell and yolk sac hematopoietic progenitors. Cell, 109, 29–37, 2002.
12) Kosaka Y., Kobayashi N., Fukazawa T., Totsugawa T., Maruyama M., Yong C., Arata T., Ikeda H., Kobayashi K., Ueda T., Kurabayashi Y., Tanaka N.: Lentivirus-based gene delivery in mouse embryonic stem cells. Artif Organs, 28, 271–277, 2004.
13) Tai G., Polak J. M., Bishop A. E., Christodoulou I., Buttery L. D.: Differentiation of osteoblasts from murine embryonic stem cells by overexpression of the transcriptional factor osterix. Tissue Eng, 10, 1456–1466, 2004.
14) Tompers D. M., Labosky P. A.: Electroporation of murine embryonic stem cells: a step-by-step guide. Stem Cells, 22, 243–249, 2004.
15) Bergelson J. M., Cunningham J. A., Droguett G., Kurt-Jones E. A., Krithivas A., Hong J. S., Horwitz M. S., Crowell R. L., Finberg R. W.: Isolation of a common receptor for Coxsackie B viruses and adenoviruses 2 and 5. Science, 275, 1320–1323, 1997.
16) Tomko R. P., Xu R., Philipson L.: HCAR and MCAR: the human and mouse cellular receptors for subgroup C adenoviruses and group B coxsackieviruses. Proc Natl Acad Sci USA, 94, 3352–3356, 1997.
17) Tontonoz P., Hu E., Spiegelman B. M.: Stimulation of adipogenesis in fibroblasts by PPAR gamma 2, a lipid-activated transcription factor. Cell, 79, 1147–1156, 1994.
18) Rosen E. D., Sarraf P., Troy A. E., Bradwin G., Moore K., Milstone D. S., Spiegelman B. M., Mortensen R. M.: PPAR gamma is required for the differentiation of adipose tissue in vivo and in vitro. Mol Cell, 4, 611–617, 1999.
19) Ducy P., Zhang R., Geoffroy V., Ridall A. L., Karsenty G.: Osf2/Cbfa1: a transcriptional activator of osteoblast differentiation. Cell, 89, 747–754, 1997.
20) Komori T., Yagi H., Nomura S., Yamaguchi A.,